Glucocorticoid receptors signaling impairment potentiates amyloid-beta oligomers-induced pathology in an acute model of Alzheimer's disease

Canet, G.; Pineau, F.; Zussy, C.; Hernandez, C.; Hunt, H.; Chevallier, N.; ... ; Givalois, L.

Received: 21 March 2019 | Revised: 5 November 2019 | Accepted: 7 November 2019

DOI: 10.1096/fj.201900723RRR

RESEARCH ARTICLE

THE FASEB JOURNAL

Glucocorticoid receptors signaling impairment potentiates amyloid-β oligomers-induced pathology in an acute model of Alzheimer's disease

Geoffrey Canet[1,2,3] | Fanny Pineau[1,2,3] | Charleine Zussy[1,2,3] | Célia Hernandez[1,2,3] | Hazel Hunt[4] | Nathalie Chevallier[1,2,3] | Véronique Perrier[1,2,3] | Joan Torrent[1,2,3] | Joseph K. Belanoff[4] | Onno C. Meijer[5] | Catherine Desrumaux[1,2,3] | Laurent Givalois[1,2,3]

[1]Molecular Mechanisms in Neurodegenerative Dementia (MMDN) Laboratory, INSERM U1198, Team Environmental Impact in Alzheimer's Disease and Related Disorders (EiAlz), Montpellier, France

[2]University of Montpellier, Montpellier, France

[3]EPHE, Paris, France

[4]Corcept Therapeutics, Menlo Park, CA, USA

[5]Einthoven Laboratory, Department of Medicine, Division of Endocrinology, Leiden University Medical Center, Leiden, The Netherlands

Correspondence
Laurent Givalois, Molecular Mechanisms in Neurodegenerative Dementia (MMDN) Laboratory, U1198 INSERM, Team Environmental Impact in Alzheimer's Disease and Related Disorders (EiAlz), Place E. Bataillon, 34095 Montpellier, France.
Email: laurent.givalois@umontpellier.fr

Funding information
Association France Alzheimer (French Alzheimer's Association), Grant/Award Number: SM2016#1512 - LG; Agence Nationale de la Recherche (ANR), Grant/Award Number: ANR-11-LABEX-0021-LipSTIC - CD; Corcept Therapeutics (Menlo Park, CA, USA), Grant/Award Number: Exceptional subvention - LG; University of Montpellier, France, Grant/Award Number: CBS2 PhD program - GC; University of Montpellier, France, Grant/Award Number: CBS2 PhD program - CH

Abstract

Dysregulation of the hypothalamic-pituitary-adrenal (HPA) axis occurs early in Alzheimer's disease (AD), associated with elevated circulating glucocorticoids (GC) and glucocorticoid receptors (GR) signaling impairment. However, the precise role of GR in the pathophysiology of AD remains unclear. Using an acute model of AD induced by the intracerebroventricular injection of amyloid-β oligomers (oAβ), we analyzed cellular and behavioral hallmarks of AD, GR signaling pathways, processing of amyloid precursor protein, and enzymes involved in Tau phosphorylation. We focused on the prefrontal cortex (PFC), particularly rich in GR, early altered in AD and involved in HPA axis control and cognitive functions. We found that oAβ impaired cognitive and emotional behaviors, increased plasma GC levels, synaptic deficits, apoptosis and neuroinflammatory processes. Moreover, oAβ potentiated the amyloidogenic pathway and enzymes involved both in Tau hyperphosphorylation and GR activation. Treatment with a selective GR modulator (sGRm) normalized plasma GC levels and all behavioral and biochemical parameters analyzed. GR seems to occupy a central position in the pathophysiology of AD. Deregulation of

Abbreviations: Aβ, amyloid-β peptide; ADAM10, A disintegrin and metalloproteinase domain-containing protein 10 (*α-secretase*); APP, amyloid precursor protein; AR, androgen receptors; BACE1, β-APP cleaving enzyme type 1 (*β-secretase*); β-tub, β-tubulin; CDK, cyclin-dependent kinases; CORT, corticosterone; EPM, elevated plus maze; GFAP, glial fibrillary acidic protein; GC, glucocorticoids; GR, glucocorticoid receptors; GRE, glucocorticoid response element; GSK-3β, glycogen synthase kinase-3β; HPA axis, hypothalamic-pituitary-adrenal axis; HSP, heat shock protein; Iba1, ionized calcium-binding adapter molecule 1; Icv, intracerebroventricular; IDE, insulin-degrading enzyme; Ip, intraperitoneal; MR, mineralocorticoid receptors; NFT, neurofibrillary tangles; $oA\beta_{25\text{-}35}$, oligomers of Aβ fragment [25-35]; PDK1, 3-phosphoinositide-dependent kinase; PFC, prefrontal cortex; PR, progesterone receptors; PS1, presenilin 1 (*α-secretase*); PSD95, postsynaptic density protein 95; ROCK, Rho-associated coiled-coil kinase; sAPPα, α-secretase-cleaved soluble APP ectodomain; sGRm, selective GR modulator; SYN, synaptotagmine; TACE, tumor necrosis factor-α-converting enzyme; TAT, tyrosine aminotransferase activity assay.

the HPA axis and a feed-forward effect on PFC GR sensitivity could participate in the etiology of AD, in perturbing Aβ and Tau homeostasis. These results also reinforce the therapeutic potential of sGRm in AD.

KEYWORDS

Cdk5, GSK-3β, PDK1, ROCK, selective GR modulator

1 | INTRODUCTION

Alzheimer's disease (AD), the most common cause of dementia in the elderly, is characterized by a progressive impairment of cognitive functions and the presence of senile plaques and neurofibrillary tangles (NFT) throughout the brain, including areas particularly involved in memory formation and emotional regulation. Plaques are composed of insoluble extracellular aggregates consisting mainly of amyloid-β (Aβ) peptides, while NFT result from hyper- and abnormal phosphorylation of the microtubule-stabilizing protein Tau.[1] There are several forms of AD. Familial forms with known mutations of specific genes represent less than 5% of cases, whereas 95% of patients develop sporadic forms, with unknown mechanisms, but with identified risk factors. The principal risk factor for sporadic AD is aging. But, there is also growing evidence that stressful lifetime events may increase the probability of developing AD.[2] This view is particularly supported by the fact that in AD patients, cognitive and psychological symptoms are associated with an early deregulation of the hypothalamic-pituitary-adrenal (HPA) axis, as well as elevated levels of glucocorticoids (GC) in plasma and CSF.[3,4]

The HPA axis, highly involved in the stress response, triggers the adrenal cortex to release GC. These steroid hormones readily cross the BBB and bind to low-affinity glucocorticoid receptors (GR) and high-affinity mineralocorticoid receptors (MR).[5] GC are necessary for normal cellular activity and fundamental for many CNS functions, including learning and memory.[6] While MR are localized mainly in the hippocampus, GR are more ubiquitous and are particularly found in several structures of the limbic system (prefrontal cortex [PFC], hippocampus, and amygdala), which are strongly involved in cognitive and psychological functions but also are important components of the neural circuitry modulating HPA axis activity.[7]

GC act synergistically with excitatory amino acids (like glutamate) in neurotoxicity. Hence, a deregulation of the HPA axis activity or a modification of GR functioning could be extremely toxic, especially in limbic structures,[8] and thus could contribute to the cognitive decline and psychological symptoms that occur in AD. In chronic animal models of AD (transgenic mice), stress and GC administration affect the course of the pathology. Chronic stress accelerates the onset of cognitive deficits, triggers amyloid precursor protein (APP) misprocessing, enhances plaque pathology, reduces Aβ clearance, increases Aβ levels, and stimulates Tau hyperphosphorylation and its neuronal accumulation.[9,10] In the same line of evidence, a recent study showed that early life stress in APP/PS1 mice induced elevated corticosterone levels, associated with enhanced hippocampal $A\beta_{1\text{-}40/42}$ and BACE1 levels.[11] In an acute pathomimetic model of AD obtained after a single intracerebroventricular (icv) injection of an oligomeric solution of Aβ ($oA\beta_{25\text{-}35}$),[12-14] we demonstrated a strong, long-lasting activation of the HPA axis, associated with a modification of GR and MR expression in brain regions involved in the control of GC secretion (hippocampus, amygdala, and hypothalamus),[15] supporting its involvement in the etiology of AD.[9,16-19] We also observed that an antagonist and selective modulators of the GR could potently counteract the effects of $oA\beta_{25\text{-}35}$ injection in the hippocampus, arguing strongly for a therapeutic potential of modulating GR activity.[14]

In the present preclinical study, we focused our attention on the PFC for several reasons. (a) It is a cerebral region highly involved in the control of the HPA axis. Indeed, the PFC is involved in both driving the stress-induced activation of the HPA axis, and in mediating negative feedback regulation in times of stress.[20] (b) The different subdivisions of the PFC are particularly involved in cognitive and emotional processing.[21] (c) In AD, the PFC is rapidly affected.[22] (d) GR levels in the PFC are fivefold higher than MR levels,[23] suggesting that the PFC could be particularly sensitive to a dysregulation of the HPA axis activity.

Thus, on the basis of our previous findings,[12-14] we took advantage of specific properties of a new selective GR modulator (sGRm) CORT113176 to decipher the role of GR in AD. CORT113176 is representative of a series of novel, selective non-steroidal GR ligands (1H-pyrazolo(3,4-g)hexahydro-isoquinoline sulfonamides) developed by *Corcept Therapeutics* (Figure 1B). It exhibits excellent affinity for GR with no measurable affinity for the other nuclear hormone receptors (progesterone, androgen, mineralocorticoid, and estrogen).[14,24-26] CORT113176 demonstrated only partial antagonism and also some agonism in reaction to a viral protein

in rat hepatocytes.[14] Hence, we refer to it as a sGRm, with the implication of the advantages linked to selective receptor modulation that we previously reported in detail.[14] In fact, this family of molecules has the potential to more selectively abrogate pathogenic GR-dependent processes in the brain (*as antagonist*), while retaining beneficial aspects of GR signaling (*as agonist*).[14,27-30]

2 | MATERIALS AND METHODS

2.1 | Animals

Adult male Sprague-Dawley rats (*Janvier Lab., Le Genest-Saint-Isle, France*) weighing 260-280 g (8 weeks), at the beginning of the experiments, were housed 1 week before

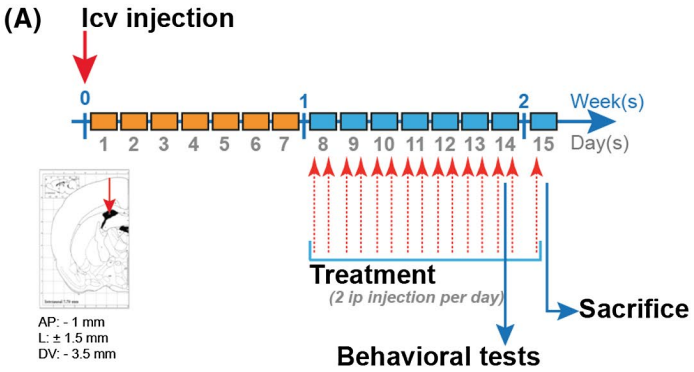

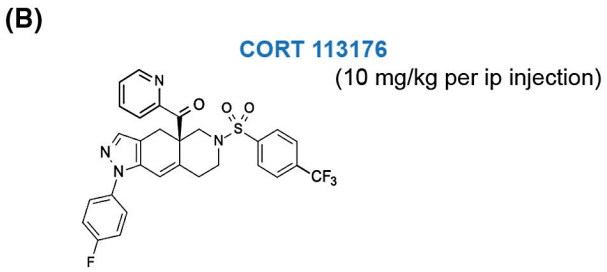

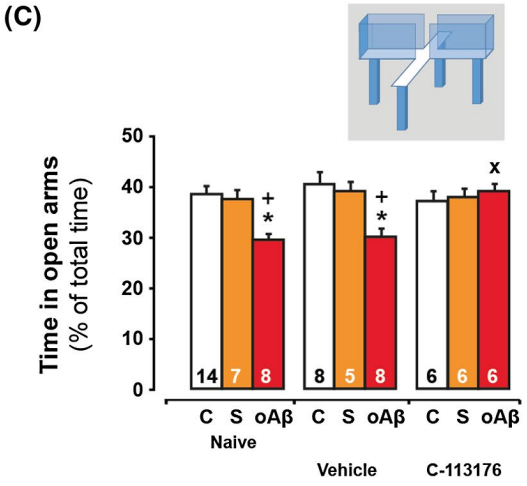

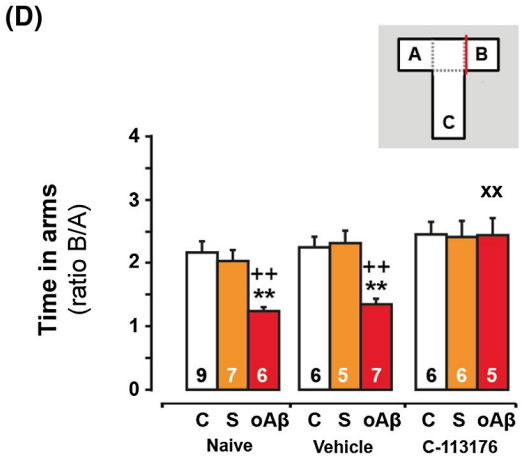

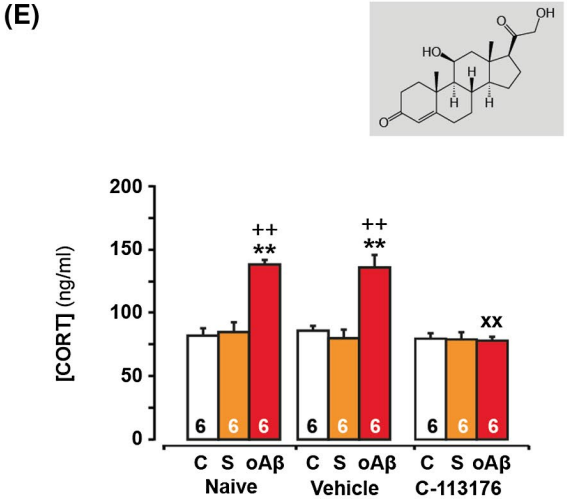

FIGURE 1 Effects of selective GR modulator on, anxious behavior, spatial short-term memory deficits and high levels of corticosterone induced by the icv injection of oA$\beta_{25\text{-}35}$. A, *Experimental protocol*—At T0, adult male rats (Sprague Dawley) were injected directly into the lateral ventricles using a stereotaxic apparatus (coordinates: AP −1 mm, L ±1.5 mm, DV −3.5 mm). One group has not undergone surgery (control rats, white column), a second group received an icv injection of scrambled A$\beta_{25\text{-}35}$ peptide (negative control—10 µg/rat—orange column) and a third group received an icv injection of oA$\beta_{25\text{-}35}$ peptide (Aβ—0 µg/rat—red column). Animals were weighted daily and one week after the icv injection (at Week 1), animals were treated with vehicle or CORT113176 (10 mg/kg per injection) through two intraperitoneal (ip) injections per day during 7 days. At day 14 (Week 2), the anxious behavior or the spatial short-term memory of each rat were tested in an elevated plus maze (EPM) or in a T-maze, respectively. The following day (day 15), 30 minutes after the last ip injection, the animals were sacrificed, blood samples and PFC were rapidly collected for corticosterone assay and Western blot analysis, respectively. B, Chemical structure of the selective GR modulator tested in this study, CORT113176 (*reproduction with the permission of Corcept Therapeutics*). C, Anxious behavior was determined in the EPM paradigm. Each animal was placed at the center of the EPM and allowed to freely explore for 10 minutes. Data were expressed as time spent in the open arms (OA) in % of total time. Two-way ANOVA: $F_{2,59} = 7.90$ for group, $P < .001$, $F_{2,59} = 1.54$ for treatment, ns; and $F_{4,59} = 2.95$ for interaction, $P < .05$. D, Spatial short-term memory performance was determined in a T-maze test and was expressed as the ratio of the time spent in the initially closed arm (B) over the time spent in the previous arm (A). Two-way ANOVA: $F_{2,48} = 9.10$ for group, $P < .001$; $F_{2,48} = 8.51$ for treatment, $P < .001$; and $F_{4,48} = 2.36$ for interaction, ns. E, Plasma concentrations of corticosterone (CORT) were determined by Elisa and expressed as ng/ml. Two-way ANOVA: $F_{2,45} = 39.0$ for group, $P < .0001$; $F_{2,45} = 15.3$ for treatment, $P < .0001$; and $F_{4,45} = 10.8$ for interaction, $P < .0001$. $^{*}P < .05$ and $^{**}P < .01$ vs respective control (C) group. $^{+}P < .05$ and $^{++}P < .01$ vs respective scrambled (S) group. $^{x}P < .05$ and $^{xx}P < .01$ vs respective naive rat in each group (C, S or oAβ). The number of animals in each group is indicated within the columns

experiments in a standard animal facility (12H/12H light/dark cycle with lights on at 07H00; 21 ± 1°C, food and water ad libitum). All experiments, including sacrifices, were performed in conscious rats between 09H00 and 14H00, during the diurnal trough of the HPA axis circadian rhythm.

2.2 | Ethical considerations

Animal procedures were conducted in strict adherence to the European Union Directive of 2010 (2010/63/EU). The National French Animal Welfare Committee and the local committee at the University of Montpellier approved all protocols (*authorization: CEEA-LR-12160*). All efforts were made to minimize the number of animals used, potential pain, suffering, and distress.

2.3 | Amyloid-β peptide

In patients, soluble Aβ oligomers contains mainly the sequences A$\beta_{1\text{-}40}$ and A$\beta_{1\text{-}42}$.[1] However, they also contain peptides with shorter sequences such as A$\beta_{25\text{-}35}$ or A$\beta_{25\text{-}35/40}$,[31-33] identical between human and rodent.[34] It can be produced in AD patients by enzymatic cleavage of A$\beta_{1\text{-}40}$.[31,32] This Aβ peptide includes extracellular and transmembrane residues that have been reported to represent a biologically active region of Aβ[35-37] and to contain the highly hydrophobic region forming stable aggregates.[36] Interest in this undecapeptide, which itself shows a β-sheet structure,[12,36] has grown over the last decade, mainly because it induces neurite atrophy, neuronal cell death, synaptic loss, as well as synaptic plasticity and memory deficits in a similar way to A$\beta_{1\text{-}40}$ and A$\beta_{1\text{-}42}$,[37] but with better solubility and efficiency.[38,39] A$\beta_{25\text{-}35}$ and scrambled A$\beta_{25\text{-}35}$ peptides (*PolyPeptide, Strasbourg, France*) were dissolved in sterile water (1 µg/µL) and stored at −20°C. Since soluble Aβ oligomers correlate better with the progression of the disease,[40] A$\beta_{25\text{-}35}$ and scrambled peptides were aggregated by in vitro incubation at 37°C (4 days) to obtain a solution mainly composed (more than 95%) of a mixture of soluble oligomer species (oA$\beta_{25\text{-}35}$), as previously characterized.[13]

2.4 | Experimental procedures

To evaluate the impact of oA$\beta_{25\text{-}35}$ (*acute model of AD*), animals were divided into three groups. One group had no surgery (control rats), a second received an icv injection of incubated scrambled peptide (10 µg/rat), and a third received an icv injection of oA$\beta_{25\text{-}35}$ (10 µg/rat). The animals were anesthetized with an intraperitoneal (ip) injection of 1 ml of a mixture of ketamine and xylazine (80 and 10 mg/kg b.w., respectively). oA$\beta_{25\text{-}35}$ was injected directly into the lateral ventricles using a David-Kopf stereotaxic apparatus (*Phymep, Paris, France*), (coordinates: AP −1 mm, L ±1.5 mm, DV −3.5 mm) (Figure 1A).[41] Based on a previous study[14] and to decipher the role of GR in oAβ toxicity, treatment with sGRm was conducted 1 week after the icv injection of oA$\beta_{25\text{-}35}$. CORT113176 (10 mg/kg b.w. per injection) (*Corcept Therapeutics, Menlo Park, CA, USA*) (Figure 1B) was injected ip twice a day (09H00 and 18H00) for 1 week. The short-term memory or anxiety state of different groups of rats were tested (day 14) in a T-maze or in an elevated plus maze test (EPM), respectively. The following day (day 15) and 30 minutes after

the last ip injection, the unanesthetized animals were sacrificed by decapitation. Blood samples and the PFC were rapidly collected for corticosterone assay and WB analysis. Naive rats received no treatment but were manipulated in the same manner as treated rats. Vehicle rats received only ip injections of sesame oil and served as negative controls for pharmacological treatments.

2.5 | Spatial short-term memory

T-maze test was used to rapidly assess the delayed alternation of rats. This memory behavioral test was used as a non-invasive recurrent readout that we usually perform to make sure we have an appropriate toxicity.[12-15] The T-maze consisted of two short arms (A and B), extending from a longer alley and enclosed with high walls. The test involved two trials separated by 1 hour. During the training session, one short arm (B) was closed. Rats were placed at the end of the long alley, allowed to visit the maze for 10 minutes and then returned into their home cage. During the test session, animals were placed in the maze for 2 minutes, with free access to all arms. The number of visits and time spent in each arm were measured. The results were expressed as ratio of the time spent in the initially closed novel arm, over the time spent in the previous arm and as a ratio of the number of entries into the novel arm over the familiar one. The apparatus was cleaned with diluted ethanol (50%) between animals.

2.6 | Anxiety behavior

The anxiety state of rats was measured using their ability to explore open and enclosed arms of an EPM, as previously described.[15] The clear plexiglass apparatus consisted of two open arms (50 × 10 cm) and two enclosed arms (50 × 10 × 45 cm high), extending from a central platform and placed 60 cm above the floor. Each rat was placed at the center of the plus-maze facing the closed arm and its exploration behavior was recorded for 10 minutes. The results were expressed as total time spent in the open arms and the total number of entries was counted to verify general motor activity. An entry into an arm was recorded if the animal crossed the line that connected that arm with the central platform with all four legs. The apparatus was cleaned with diluted ethanol (50%) between animals.

2.7 | Corticosterone assay

Blood samples were collected at the time of sacrifice (day 15), on 1 mg/mL EDTA (*Sigma-Aldrich, Saint Quentin Fallavier, France*), centrifuged at 4°C, and plasma stored at −20°C until assayed for corticosterone.[14] Plasma corticosterone concentrations were assayed using a conventional ELISA kit (*Enzo-Life Sciences, Farmingdale, NY, USA*) in a 10-µL plasma sample diluted (1:40) with the assay buffer. The assay sensitivity was 27 pg/mL. The intra- and inter-assay coefficients were 6.6% and 7.8%, respectively.

2.7.1 | $A\beta_{1\text{-}42}$ assay

Rats were sacrificed by decapitation 15 days after $oA\beta_{25–35}$ injection and brains were rapidly removed, PFC dissected out, weighted, frozen in liquid nitrogen, and stored at −80°C until assayed. After thawing, PFC were sonicated (*VibraCell; Sonics & Materials, Newtown, CT, USA*) for 20 seconds in a lysis buffer.[42] After centrifugation (14 000 rpm for 25 minutes, 4°C), supernatants were used for $A\beta_{1\text{-}42}$ ELISA assay (*Anaspec, Fremont, CA, USA*), according to the manufacturer's instructions. Absorbance was read at 450 nm (*Tecan i-control, ThermoFisher Scientific, Illkirch, France*) and sample concentration was calculated using the standard curve (Figure S3A). Results were then expressed in pg of $A\beta_{1\text{-}42}$/g of tissue. The assay sensitivity was 3.91 pg/mL. The intra- and inter-assay coefficients were 4.3% and 6.4%, respectively.

2.8 | WB analysis

WB were performed as previously described[14] in the whole PFC. All antibodies used are detailed in the Table 1. Briefly, after sacrifice, the PFC was micro-dissected, weighed, immediately frozen on liquid nitrogen and stored at −20°C. Tissues were sonicated (*VibraCell; Sonics & Materials, Newtown, CT, USA*) in a lysis buffer[12] and centrifuged (4°C). Supernatants were collected and the protein concentration was measured using a BCA kit (*ThermoFisher Scientific, Illkirch, France*). In all, 60 µg from each sample was taken for WB analysis. Samples were separated in SDS-polyacrylamide gel (12%) and transferred to a PVDF membrane (*Merck-Millipore, Dachstein, France*). The membrane was incubated overnight (4°C) with the primary antibody, rinsed and then incubated for 2 hours with the appropriate horseradish peroxidase-conjugated secondary antibody. Peroxidase activity was revealed using enhanced-chemiluminescence (ECL) reagents (*Luminata-Crescendo, Merck-Millipore*). The intensity of peroxidase activity was quantified using Image-J software (*NIH, Bethesda, MA, USA*). β-tubulin (β-Tub) was used as a loading control for all immunoblotting experiments.

2.9 | Statistical analysis

Data are presented as mean ± SEM and analyzed using two-way ANOVA followed by a Tukey's multiple comparison

TABLE 1 Antibodies used in Western blot experiments

Protein	Mol. weight	Antibody	Dilution	Ref.	Supplier
Primary antibodies					
ADAM10[85]	72 kDa	Rabbit anti-ADAM10	1/1000	AB19026	Merck-Millipore, France
APP/C99[14]	125/13 kDa	Rabbit anti-APP/C99	1/750	PA1-84165	Thermo-Fisher Scientific, France
BACE1[14]	70 kDa	Rabbit anti-BACE	1/1000	#5606	Cell Signaling/Ozyme,, St Cyr-l'Ecole, France
Calpain 1[86]	80 kDa	Rabbit anti-calpain 1 large subunit (μ-type)	1/1000	#2556	Cell Signaling/Ozyme, France
Caspase 3[14]	19 kDa	Rabbit anti-caspase 3	1/500	#9665	Cell Signaling/Ozyme, France
Cdk5[87]	30 kDa	Rabbit anti-Cdk5	1/500	#2506	Cell Signaling/Ozyme, France
Fyn[88]	59 kDa	Rabbit anti-Fyn	1/500	#4023	Cell Signaling/Ozyme, France
GFAP[14]	55 kDa	Mouse anti-GFAP	1/2000	G3893	Sigma-Aldrich, France
GR[15]	95 kDa	Rabbit anti-GR	1/1000	#3660	Cell Signaling/Ozyme, France
GSK-3β[39]	46 kDa	Mouse anti-GSK-3β	1/2000	610202	BD-Biosciences, Rungis, France
HSP70[34]	70 kDa	Rabbit anti-HSP70	1/500	#4872	Cell Signaling/Ozyme, France
HSP90[34]	90 kDa	Rabbit anti-HSP90	1/1000	#4877	Cell Signaling/Ozyme, France
Iba1[14]	17 kDa	Rabbit anti-Iba1	1/750	013-19741	Wako Chem, Osaka, Japan
IDE[14]	110 kDa	Rabbit anti-IDE	1/3000	AB9210	Merck-Millipore, France
MR[15]	100 kDa	Rabbit anti-MR	1/100	SC11-412	SantaCruz Biotech., Dallas, TX, USA
p[Ser9] GSK-3β[39]	46 kDa	Mouse anti-p[Ser9]GSK-3β	1/1000	#9336	Cell Signaling/Ozyme, France
p[Tyr211] GSK-3β[39]	46 kDa	Mouse anti-p[Tyr216] GSK-3β	1/2000	612313	BD-Biosciences, France
p35/p25[87]	35/25 kDa	Rabbit anti-p35/p25	1/500	#2680	Cell Signaling/Ozyme, France
PDK1[58]	56-68 kDa	Rabbit anti-PDK1	1/1000	#5662	Cell Signaling/Ozyme, France
pGR[89]	95 kDa	Rabbit anti-p[Ser211]GR	1/1000	#4161	Cell Signaling/Ozyme, France
PS1[90]	22 kDa	Rabbit anti-PS1	1/1000	#5643	Cell Signaling/Ozyme, France
PSD95[14]	95 kDa	Rabbit anti-PSD95	1/2000	#3450	Cell Signaling/Ozyme, France
ROCK1[58]	160 kDa	Rabbit anti-ROCK1	1/500	#4035	Cell Signaling/Ozyme, France
ROCK2 [58]	160 kDa	Rabbit anti-ROCK2	1/500	#8236	Cell Signaling/Ozyme, France
sAPPα[58]	100 kDa	Mouse anti-sAPPα	1/50	11098	IBL, Hamburg, Germany
SYN[14]	65 kDa	Mouse anti-synaptotagmine	1/1000	MAB5200	Merck-Millipore, France
β-Tub	50 kDa	Mouse anti-β-Tubulin	1/7500	T4026	Sigma-Aldrich, France
Secondary antibodies					
IgG	Goat anti-rabbit IgG peroxidase conjugate		1/2000	A61-54	Sigma-Aldrich, France
IgG	Goat anti-mouse IgG peroxidase conjugate		1/2000	A67-82	Sigma-Aldrich, France

test (*GraphPad-Prism 5.0*). $P < .05$ was considered significant. The number of animals in each group is indicated within the columns. Before each analysis of variance, the Gaussian distribution was evaluated and validated by a Kolmogorov-Smirnov test (*GraphPad-Prism 5.0*).

3 | RESULTS

To characterize the impact of oA$\beta_{25\text{-}35}$, we previously tested over time (*after 1 and 2 weeks*) two different doses (5 and 10 μg/rat) on several parameters previously characterized in this acute model of AD[12] (Figure S1A). While the scrambled peptide induced no modification in comparison with control naive rats, the dose of 10 μg of oA$\beta_{25\text{-}35}$ was more efficient than the dose of 5 μg. Indeed, after 10 μg short-term memory deficit (T-maze) was observed up to 2 weeks post-injection (Figure S1B) and plasma levels of corticosterone were increased from 1 to 2 weeks (Figure S1C).

We next evaluated (in the PFC) the role of GR in the oAβ toxicity using a sGRm (CORT113176). Animals were treated 1 week after the icv injection of oA$\beta_{25\text{-}35}$ with CORT113176

according to a protocol and a dose established in a previous study.[14] Control scrambled peptide and vehicle treatment induced no changes in any of the readouts relative to untreated animals (Figures 1-6). All blots of control conditions were presented in a supplementary document (Figure S2) to improve the clarity of figures and to highlight key effects. Two weeks after oAβ_{25-35}, animals presented anxious behavior (Figure 1C), short-term memory deficits (Figure 1D), and high plasma concentrations of corticosterone (Figure 1E). Treatment with CORT113176 reversed all of these parameters (Figure 1).

Behavioral deficits, observed 2 weeks after oAβ_{25-35}, were associated with pre- (SYN) and post-synaptic (PSD95) deficits, increased apoptotic marker expression (Figure 2A-D) and a marked neuroinflammation characterized by the activation of astrocytes (GFAP) (Figure 2A,E) and microglial cells (Iba1) (Figure 2A,F). Treatment with the sGRm normalized Caspase 3 expression, the pre- and post-synaptic deficits (Figure 2A,C,D) and blocked the neuroinflammatory processes (Figure 2A,F), as previously reported at the hippocampus level[14] or at the spinal cord level in an experimental model of amyotrophic lateral sclerosis.[30]

To determine in the PFC the effects of oAβ_{25-35} (and of CORT113176) on glucocorticoid receptor signaling, as part of a potential feed-forward or feedback process, animals were treated as previously detailed (Figure 1A). The icv injection of oAβ_{25-35} increased the expression of MR and GR (Figure 3A-C). These effects were associated with an over-activation of GR, as characterized by an increase in the phosphorylated form of GR (Ser^{211}) (Figure 3A,D). There were opposite changes in the expression of HSP90 and HSP70, the two main chaperones involved in the activity of GR,[43] but also involved in the control of Aβ and Tau aggregation.[44-46] The HSP90/HSP70 ratio (which reflects GR activation)[43] accordingly was substantially increased (Figure 3A,E). Treatment with CORT113176 reversed the increase in GR and MR, decreased the phosphorylation of GR and normalized the HSP90/HSP70 ratio (Figure 3).

The GR phosphorylation status[47] may constitute an important link between AD and GC. Indeed, GR can be phosphorylated on several serine and threonine residues. Thus, we characterized the impact of oAβ_{25-35} on GSK-3β and Cdk5, the two main enzymes involved in both the phosphorylation of GR[48] and the hyperphosphorylation of Tau.[49,50] We first confirmed changed expression ratios of p(Ser9)GSK-3β/GSK-3β and p(Tyr216)GSK-3β/GSK-3β[51] (Figure 4A-C), reflecting an increase in GSK-3β activation. Second, we observed increased levels of Cdk5 (Figure 4A,D), in association with those of p35 and p25, which are involved in Cdk5 activation[52] (Figure 4A,E). We also measured increased levels of Calpain 1, a member of cysteine proteases family regulated by intracellular calcium and showing aberrant activity in AD.[53] Calpain 1 is particularly involved in the activation of GSK-3β,[54] and in the maturation of p35 in p25[55] (Figure 4A,F). Lastly, we observed increases in the levels of Fyn (Figure 4A,G), a Src kinase associated with non-genomic effects of GR,[56] involved in the activation of GSK-3β and the phosphorylation of Tau.[49,57] This family of enzymes is bound to the inactive form of GR as chaperone, and released when GC bind to their receptors.[56] Under physiological conditions, GC inhibit Fyn activity and phosphorylation,[58] but under chronic stress, with high levels of GC, Fyn is upregulated especially in the hippocampus of adult rats.[59] To summarize, the icv injection of oAβ_{25-35} activated both GSK-3β and Cdk5 pathways. This activation was associated with an increase in p25, Calpain 1, and Fyn levels in the PFC (Figure 4). Treatment with CORT113176 inhibited the activation of GSK-3β and Cdk5, the maturation of p35 into p25 and the increase in Calpain 1 and Fyn (Figure 4).

In the next part of this study, we characterized the different pathways of APP maturation, through the assessment of the different cellular elements involved in the mutually exclusive processing pathways of APP, the amyloidogenic and non-amyloidogenic pathways (Figures 5 and 6). APP processing and induction of the amyloidogenic pathway (Figure 5) were evaluated by measuring PFC levels of full-length APP (*precursor of amyloid proteins*) (Figure 5A,B), C99 (*precursor of Aβ peptides*) (Figure 5A,C), BACE1 (*β-APP cleaving enzyme*) (Figure 5A,D), PS1 (*presenilin-1, a subunit of the γ-secretase*) (Figure 5A,E), and IDE (*insulin-degrading enzyme, involved in the clearance of Aβ*) (Figure 5A,F). Two weeks after the injection of oAβ_{25-35}, APP levels were increased and amyloidogenic processing was enhanced. This activation was associated with an increased formation (BACE1 and PS1), and a decreased clearance (IDE). One week of treatment with CORT113176 inhibited the activation of the amyloidogenic pathway. The increase in levels of APP, C99, PS1, and BACE1 and also the IDE downregulation were fully reversed (Figure 5). To characterize the non-amyloidogenic pathway in the PFC, we evaluated by Western blot the levels of the α-secretase-cleaved soluble APP ectodomain (sAPPα) and ADAM10 (*A disintegrin and metalloproteinase Domain-containing protein 10, a component of α-secretase*) (Figure 6A-C). Two weeks after the injection of oAβ_{25-35}, sAPPα and ADAM10 were decreased. This inhibition of the non-amyloidogenic processing of APP was totally reversed by 1 week of treatment with CORT113176 (Figure 6A-C). Finally, to confirm the induction of the amyloidogenic pathway, we assayed the endogenous levels of Aβ_{1-42} in the PFC (Figure S3). As expected, 2 weeks after the icv injection of oAβ_{25-35}, Aβ_{1-42} levels were increased by 18% in the PFC. This upregulation was totally reversed by the treatment with CORT113176 (Figure S3B). Even if the levels of Aβ_{1-42} assayed in the PFC were relatively low, they are consistent with some previous studies in rats.[60,61]

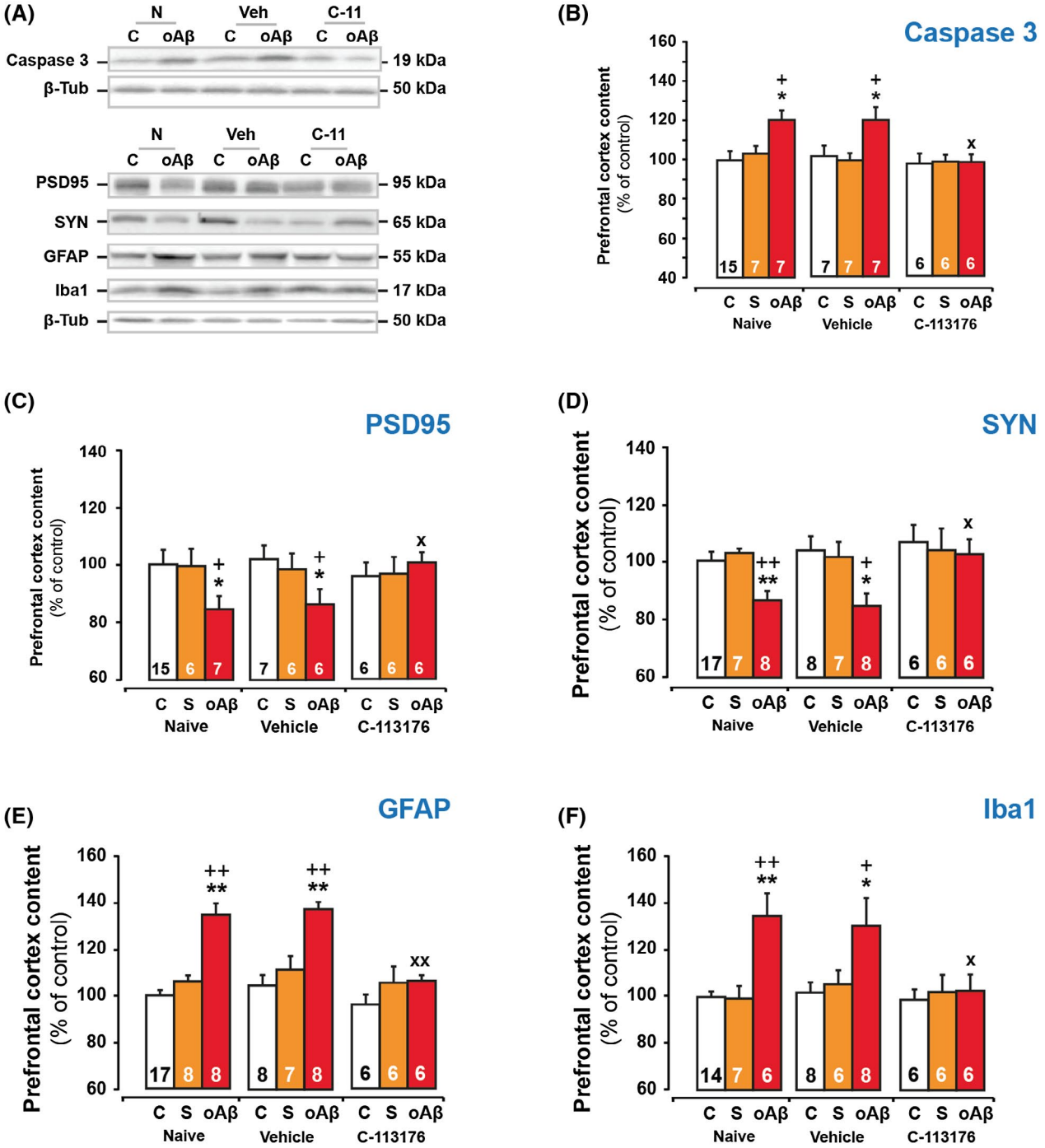

FIGURE 2 The effects in the PFC of selective GR modulator on the different cellular markers. A, modified by the icv injection of oA$\beta_{25\text{-}35}$, were evaluated by Western blot. Variations of apoptosis (caspase-3, 19 kDa) (A,B), post-synaptic marker (PSD95, 95 kDa) (A,C), pre-synaptic marker synaptotagmine (SYN, 65 kDa) (A,D), neuroinflammatory markers GFAP (55 kDa, astrocyte cells) (A,E), and Iba1 (17 kDa, microglial cells) (A,F) were evaluated in control (C—white column) and in icv injected rats with 10 µg/rat of scrambled peptide (S—orange column) or oA$\beta_{25\text{-}35}$ (Aβ—red column), treated or not with vehicle (sesame oil) or selective GR modulator, CORT113176 (10 mg/kg per ip injection). For experimental protocol, see Figure 1A. The variations of Caspase-3, PSD95, SYN, Iba1, and GFAP in the PFC were normalized with the variations of β-tubulin (β-tub, 50 kDa) and compared with non-injected rats (control group: C). Two-way ANOVA: *Caspase-3*: $F_{2,59} = 6.75$ for group, $P < .01$; $F_{2,59} = 3.08$ for treatment, $P < .05$; and $F_{4,59} = 1.73$ for interaction, ns; *PSD95*: $F_{2,67} = 4.08$ for group, $P < .05$; $F_{2,67} = 0.50$ for treatment, ns; and $F_{4,67} = 3.15$ for interaction, $P < .05$; *SYN*: $F_{2,66} = 5.97$ for group, $P < .01$; $F_{2,66} = 2.36$ for treatment, ns; and $F_{4,66} = 3.87$ for interaction, $P < .05$; *GFAP*: $F_{2,66} = 31.04$ for group, $P < .0001$; $F_{2,66} = 8.52$ for treatment, $P < .001$; and $F_{4,66} = 3.49$ for interaction, $P < .05$; *Iba1*: $F_{2,59} = 10.1$ for group, $P < .001$; $F_{2,59} = 4.28$ for treatment, $P < .05$; and $F_{4,59} = 2.08$ for interaction, ns. The variations are expressed as means ± SEM in % of control values. *$P < .05$ and **$P < .01$ vs respective control (C) group. $^{+}P < .05$ and $^{++}P < .01$ vs respective scrambled (S) group. $^{x}P < .05$ and $^{xx}P < .01$ vs respective naive rat in each group (C, S or Aβ)

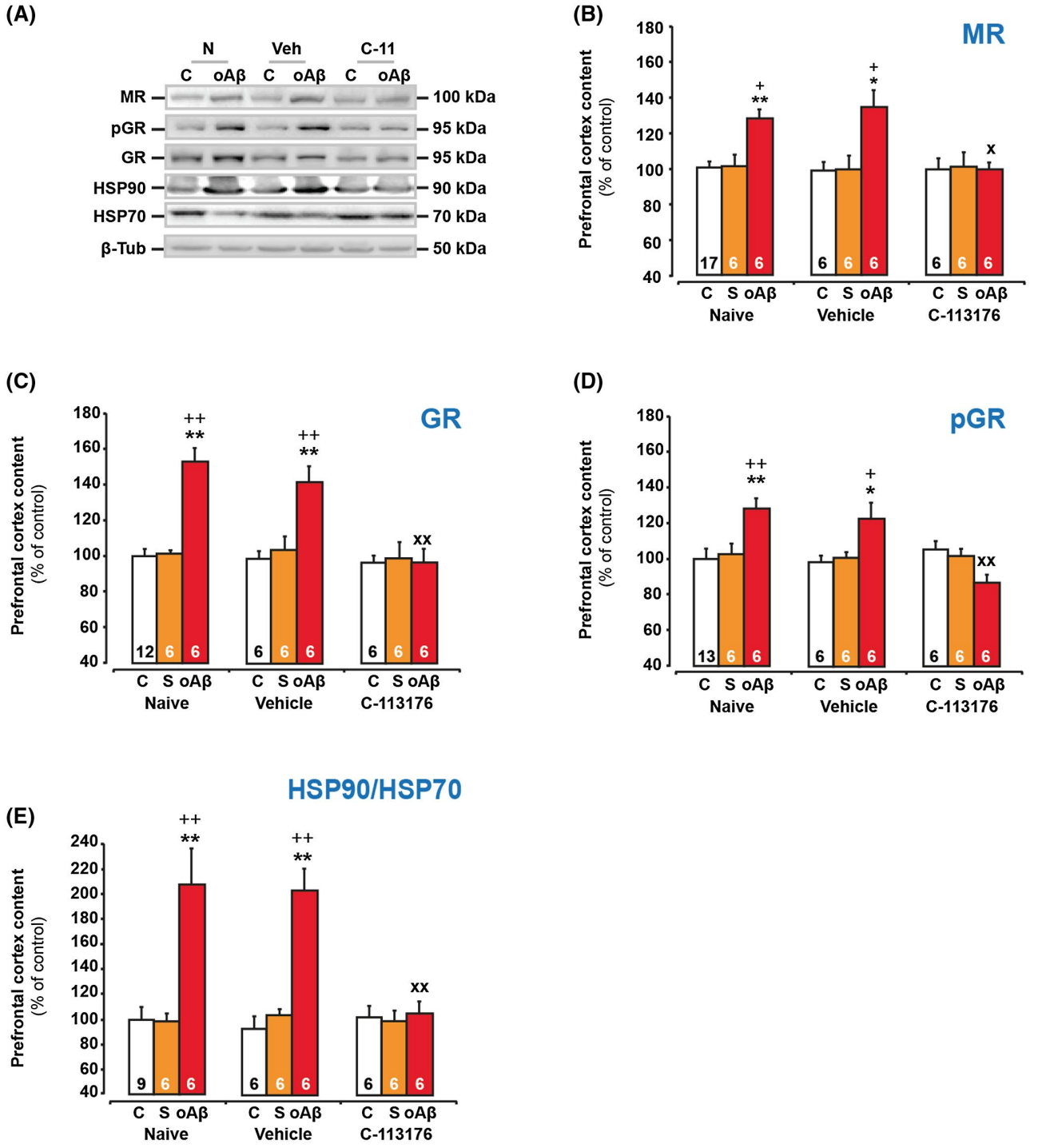

FIGURE 3 The effects in the PFC of CORT113176 on the activation of GR induced by the icv injection of oA$\beta_{25\text{-}35}$ were evaluated by Western blot. Variations of the expression of MR (100 kDa) (A,B) and GR (95 kDa) (A,C), the phosphorylation of GR (p[Ser211]GR, 95 kDA) (A,D), and the expression ratio of HSP90/HSP70 (90/70 kDa) (A,E) were evaluated in control (C—white column) and in icv injected rats with 10 µg/rat of scrambled peptide (S—orange column) or oA$\beta_{25\text{-}35}$ (Aβ—red column), treated or not with vehicle (sesame oil) or the selective GR modulator CORT113176 (10 mg/kg per ip injection). For experimental protocol, see Figure 1A. The variations of all proteins in the PFC were normalized with the variations of β-tubulin (β-tub, 50 kDa) and compared with non-injected rats (control group: C). Two-way ANOVA: *MR*: $F_{2,54} = 11.0$ for group, $P < .0001$; $F_{2,54} = 2.96$ for treatment, $P < .05$; and $F_{4,54} = 3.06$ for interaction, $P < .05$; *GR*: $F_{2,51} = 22.1$ for group, $P < .0001$; $F_{2,51} = 8.45$ for treatment, $P < .001$; and $F_{4,51} = 5.97$ for interaction, $P < .001$; *pGR*: $F_{2,52} = 2.99$ for group, $P < .05$; $F_{2,52} = 2.56$ for treatment, ns; and $F_{4,52} = 4.05$ for interaction, $P < .01$; *HSP90/HSP70*: $F_{2,50} = 29.9$ for group, $P < .0001$; $F_{2,50} = 6.00$ for treatment, $P < .01$; and $F_{4,50} = 6.55$ for interaction, $P < .001$. The variations are expressed as means ± SEM in % of control values. *$P < .05$ and **$P < .01$ vs respective control (C) group. $^{+}P < .05$ and $^{++}P < .01$ vs respective scrambled (S) group. $^{x}P < .05$ and $^{xx}P < .01$ vs respective naive rat in each group (C, S or Aβ)

To understand by which mechanisms non-amyloidogenic pathways could be inhibited, we evaluated the involvement of the Rho-kinases system. These Ser/Thr kinases are involved in cell motility, cell proliferation, autophagy, and apoptosis.[62-64] They have been suggested as potential therapeutic targets for neurodegenerative diseases, including AD.[66-68] This effect seems to be mediated by Rho-associated coiled-coil kinases (ROCK)-induced overactivation of the 3-phosphoinositide-dependent kinase 1 (PDK1) activity.[65,68] In fact, exacerbated ROCK activity

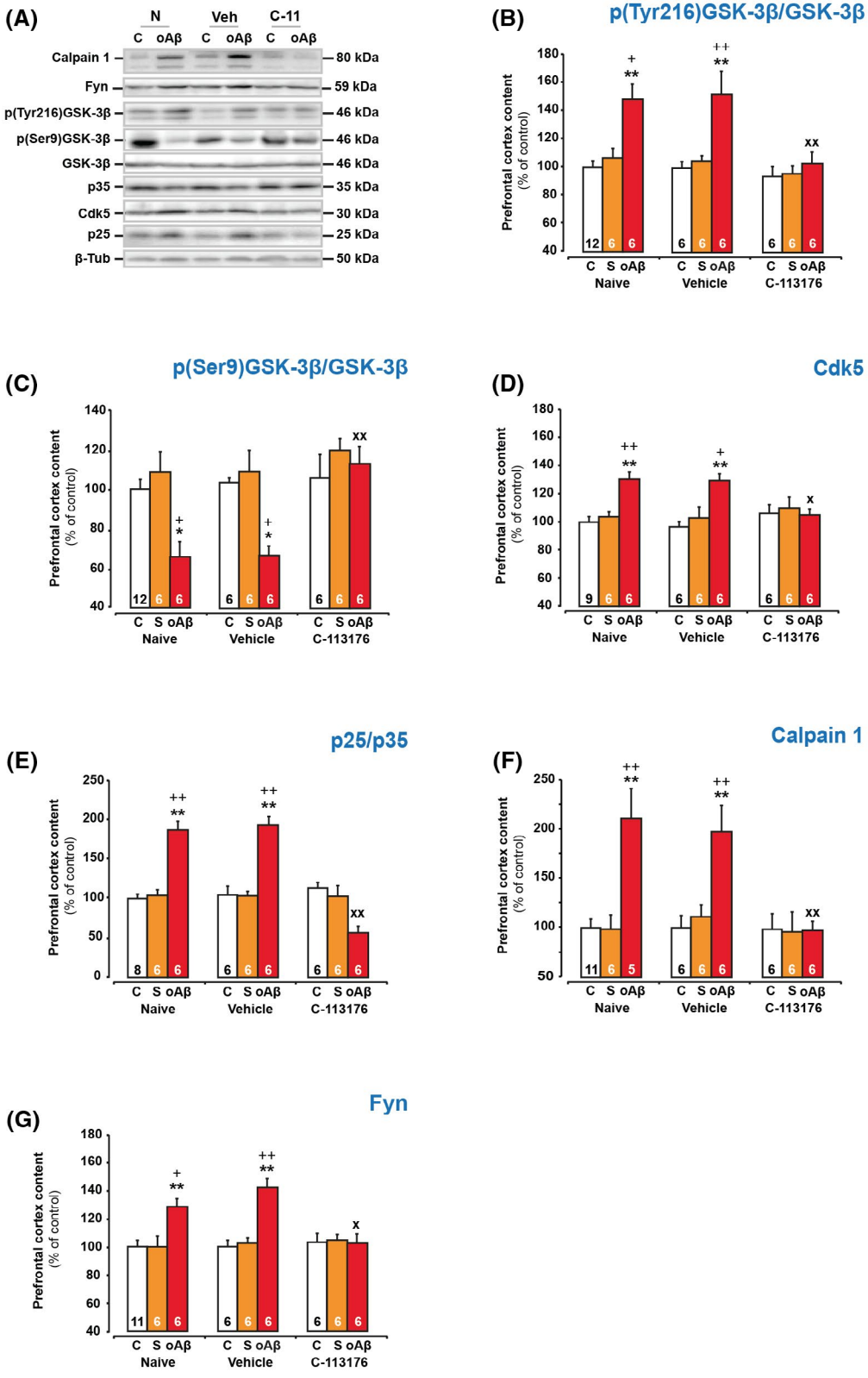

FIGURE 4 The effects in the PFC of CORT113176 on the activation of GSK-3β and Cdk5 pathways induced by the icv injection of oA$\beta_{25\text{-}35}$ were evaluated by Western blot. The activation of GSK-3β (ratio of p[Tyr216]GSK-3β/GSK-3β total & ratio of p[Ser9]GSK-3β/GSK-3β total, 46kDa each) (A-C) and Cdk5 (30 kDa) (A,D) pathways, the expression ratio of p25/p35 (25 & 35 kDa) (A,E), Calpain 1 (80 kDa) (A,F) and FYN (59 kDa) (A,G) were evaluated in control (C—white column) and in icv injected rats with 10 μg/rat of scrambled peptide (S—orange column) or oA$\beta_{25\text{-}35}$ (Aβ—red column), treated or not with vehicle (sesame oil) or the selective GR modulator CORT113176 (10 mg/kg per ip injection). For experimental protocol, see Figure 1A. The variations of all proteins in the PFC were normalized with the variations of β-tubulin (β-tub, 50 kDa) and compared with non-injected rats (control group: C). Two-way ANOVA: p[Tyr216]*GSK-3β/GSK-3β*: $F_{2,51} = 17.0$ for group, $P < .0001$; $F_{2,51} = 6.07$ for treatment, $P < .01$; and $F_{4,51} = 2.49$ for interaction, $P < .05$; p[Ser9]*GSK-3β/GSK-3β*: $F_{2,51} = 11.9$ for group, $P < .0001$; $F_{2,51} = 6.99$ for treatment, $P < .01$; and $F_{4,51} = 2.81$ for interaction, $P < .05$; *Cdk5*: $F_{2,48} = 12.1$ for group, $P < .0001$; $F_{2,48} = 0.87$ for treatment, ns; and $F_{4,48} = 3.73$ for interaction, $P < .01$; *p25/p35*: $F_{2,47} = 13.\ 2$ for group, $P < .0001$; $F_{2,47} = 12.1$ for treatment, $P < .0001$; and $F_{4,47} = 16.5$ for interaction, $P < .0001$; *Calpain 1*: $F_{2,49} = 15.5$ for group, $P < .0001$; $F_{2,49} = 5.54$ for treatment, $P < .01$; and $F_{4,49} = 4.10$ for interaction, $P < .01$; *Fyn*: $F_{2,50} = 16.1$ for group, $P < .0001$; $F_{2,50} = 2.82$ for treatment, $P < .05$; and $F_{4,50} = 4.70$ for interaction, $P < .01$. The variations are expressed as means ± SEM in % of control values. *$P < .05$ and **$P < .01$ vs respective control (C) group. $^{+}P < .05$ and $^{++}P < .01$ vs respective scrambled (S) group. $^{x}P < .05$ and $^{xx}P < .01$ vs respective naive rat in each group (C, S or Aβ). The number of animals in each group is indicated within the columns

seems to increase the pool of PDK1 molecules physically interacting with and phosphorylated by ROCK.[65,68] The overactivation of this system inhibits the non-amyloidogenic pathway [65,68] and affects Tau phosphorylation.[69,70] They seem particularly involved in the inhibition of sAPPα synthesis[68] and in the phosphorylation of Tau.[69,71] Their activity is modulated by GC[72] via GR activation.[73] To characterize the Rho-kinase system, we measured the PFC levels of Rho-associated coiled-coil kinases (ROCK1 & ROCK2) (Figure 6A,D,E) and the 3-phosphoinositide-dependent kinase (PDK1) (Figure 6A,F). Here, 2 weeks after injection of oA$\beta_{25\text{-}35}$, we observed in the PFC an increase in ROCK1, ROCK2, and PDK1, which was normalized by 1 week of treatment with the sGRm (Figure 6A,D-F).

4 | DISCUSSION

In previous studies, we provided evidence for a vicious cycle between AD and the HPA axis. We showed that the pathology, and especially the amyloid toxicity, rapidly increases GC secretion that, in turn, modulates APP processing.[14,15] This dysregulation seems to be under the control of GR, since treatment with a new class of selective GR ligands blocks the installation of this cycle in the hippocampus and re-establishes all parameters analyzed and disturbed by the amyloid toxicity (*memory and synaptic deficits, neuroinflammation, apoptosis, APP processing, and high levels of GC*).[14] This recent study[14] allowed us to design and validate the experimental protocol of treatment with sGRm. Briefly, we determined treatment timing and duration, doses and specificities of the two sGRm (*CORT108297 & CORT113167*) tested, in comparison to the non-selective antagonist of reference, Mifepristone. It appeared that 1 week of treatment (*two ip injection per day*) with CORT113176 (*10 mg/kg per injection*) displayed the most effective therapeutic potential against toxicity induced by oA$\beta_{25\text{-}35}$. Owing to its efficacy and selectivity, this sGRm was selected in the present mechanistic study.

Here, on the basis of our precedent finding,[14] we aimed to decipher the role of GR in AD and to characterize associated underlying mechanisms. For this purpose, we evaluated the impact of oA$\beta_{25\text{-}35}$ on several intracellular pathways involved in the activation of GR but also in the pathophysiology of AD. We show the establishment of several intracellular vicious cycles involving GC and GR, providing mechanistic insight to a central role of these receptors in the etiology of AD (Figure 7). The notion of a vicious cycle between GC signaling and pathogenesis is reinforced by the fact that modulation of GR activity with CORT113176 normalized all changes induced by the amyloid toxicity.

In the first part of our study, to validate our protocols in comparison with the previous study,[14] we confirmed that 1 week of treatment with a sGRm (CORT113176) at the dose of 10 mg/kg is sufficient to reverse short-term memory deficits and to re-establish plasma concentrations of corticosterone disrupted by the icv injection of oA$\beta_{25\text{-}35}$. In addition, and for the first time, we show that treatment with sGRm is able to reverse anxious behavior induced by the amyloid toxicity.[15] We equally demonstrate that sGRm treatment is able to reverse synaptic deficits, neuroinflammation, and apoptosis processes induced by oA$\beta_{25\text{-}35}$ in the PFC, as previously observed in the hippocampus.[14]

Then, we showed that the icv injection of oA$\beta_{25\text{-}35}$ increased GR phosphorylation on Ser^{211}, a site involved in the activation of GR in rats.[48] This activation was associated with an increase and activation of GSK-3β and Cdk5, with a substantial increase in the HSP90/HSP70 ratio (*important for GR activity*[43]), but also, importantly, in the control of Aβ and Tau aggregation.[44-46] The activation of GSK-3β and Cdk5 is under the control of several enzymes,[49,50,54,55,57] including Fyn and Calpain 1 that are regulated by GC,[58,59] induced by the amyloid toxicity, and

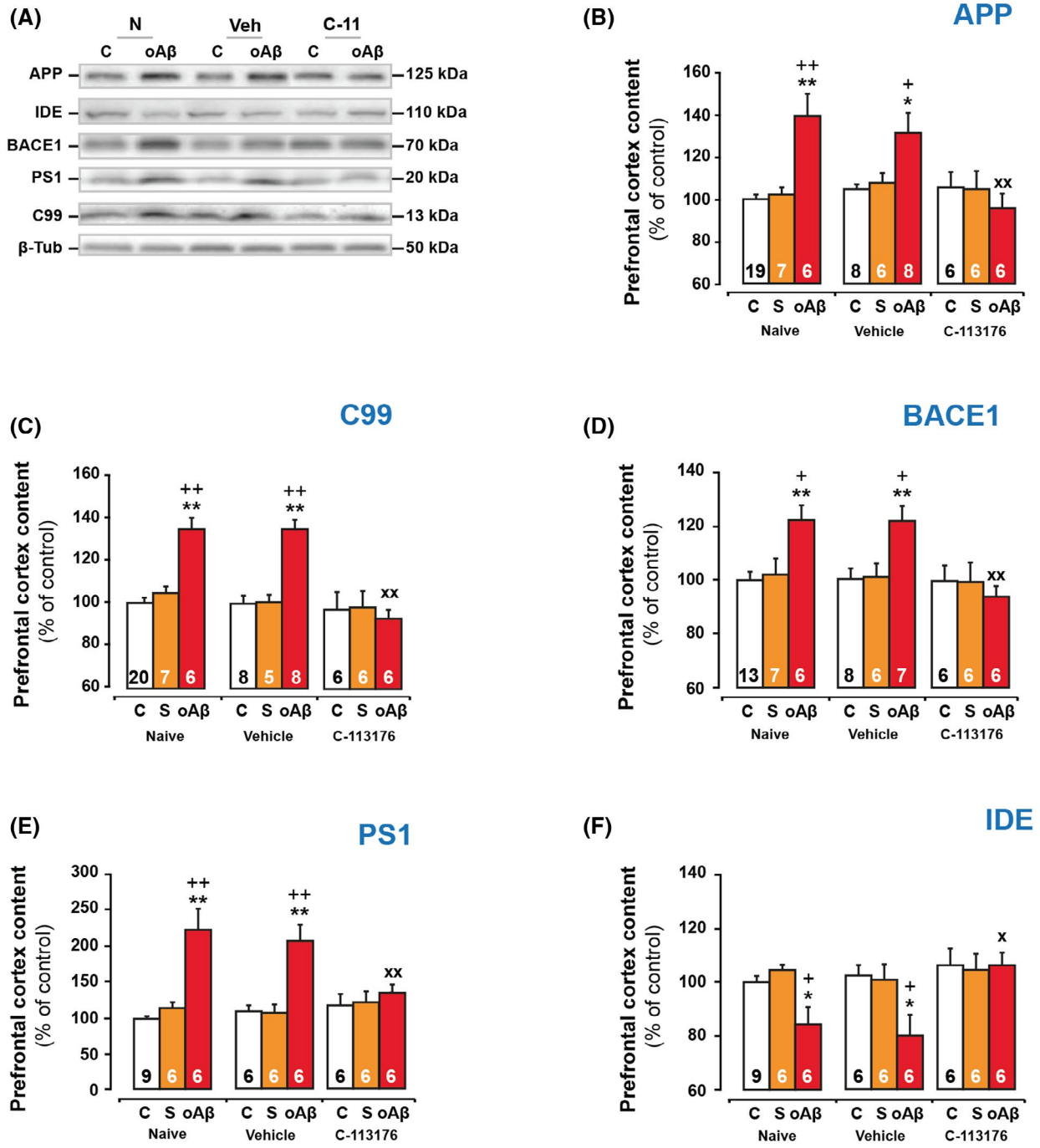

FIGURE 5 The effects in the PFC of selective GR modulator on the APP processing and the induction of the amyloidogenic pathway (A) induced by the icv injection of $oA\beta_{25\text{-}35}$ were evaluated by Western blot. Variations of full-length APP (precursor of amyloid peptides, 125 kDa) (A,B), C99 (precursor of amyloid-β peptides, 13 kDa) (A,C), β-APP cleaving enzyme (BACE1, 70 kDa) (A,D), Presenilin 1 (PS1, 20 kDa) (A,E), and insulin-degrading enzyme (IDE, 110 kDa) (A,F) were evaluated in control (C—white column) and in icv injected rats with 10 μg/rat of scrambled peptide (S—orange column), or $oA\beta_{25\text{-}35}$ (Aβ—red column), treated or not with vehicle (sesame oil) or selective GR modulator, CORT113176 (10 mg/kg per ip injection). For experimental protocol, see Figure 1A. The variations of APP, C99, BACE1, PS1, and IDE in the PFC were normalized with the variations of β-tubulin (β-tub, 50 kDa) and compared with non-injected rats (control group: C). Two-way ANOVA: *APP*: $F_{2,66} = 7.76$ for group, $P < .001$; $F_{2,66} = 3.20$ for treatment, $P < .05$; and $F_{4,66} = 4.60$ for interaction, $P < .01$; *C99*: $F_{2,56} = 21.1$ for group, $P < .0001$; $F_{2,56} = 11.5$ for treatment, $P < .0001$; and $F_{4,56} = 7.12$ for interaction, $P < .001$; *BACE1*: $F_{2,58} = 5.59$ for group, $P < .01$; $F_{2,58} = 3.99$ for treatment, $P < .05$; and $F_{4,58} = 2.92$ for interaction, $P < .05$; *PS1*: $F_{2,51} = 29.4$ for group, $P < .0001$; $F_{2,51} = 1.61$ for treatment, ns; and $F_{4,51} = 4.89$ for interaction, $P < .01$; *IDE*: $F_{2,56} = 6.47$ for group, $P < .01$; $F_{2,56} = 4.06$ for treatment, $P < .05$; and $F_{4,56} = 1.99$ for interaction, ns. The variations are expressed as means ± SEM in % of control values. $^{*}P < .05$ and $^{**}P < .01$ vs respective control (C) group. $^{+}P < .05$ and $^{++}P < .01$ vs respective scrambled (S) group. $^{x}P < .05$ and $^{xx}P < .01$ vs respective naive rat in each group (C, S or Aβ)

increased in AD patients.[74] Our data show that the overactivation of GR induced by oAβ_{25-35} coincided with an increase in these two enzymes (Figure 7).

We also observed that oAβ_{25-35} induced a strong increase in Calpain 1. This augmentation could be the reflection of its proteolytic activity, given that it was concomitant with an activation of two of its substrates, GSK-3β and an increase in p25/p35 ratio. These effects were reversed by treatment with the sGRm (CORT113176), providing evidence of an intracellular loop by which pathology increases the activation of GR

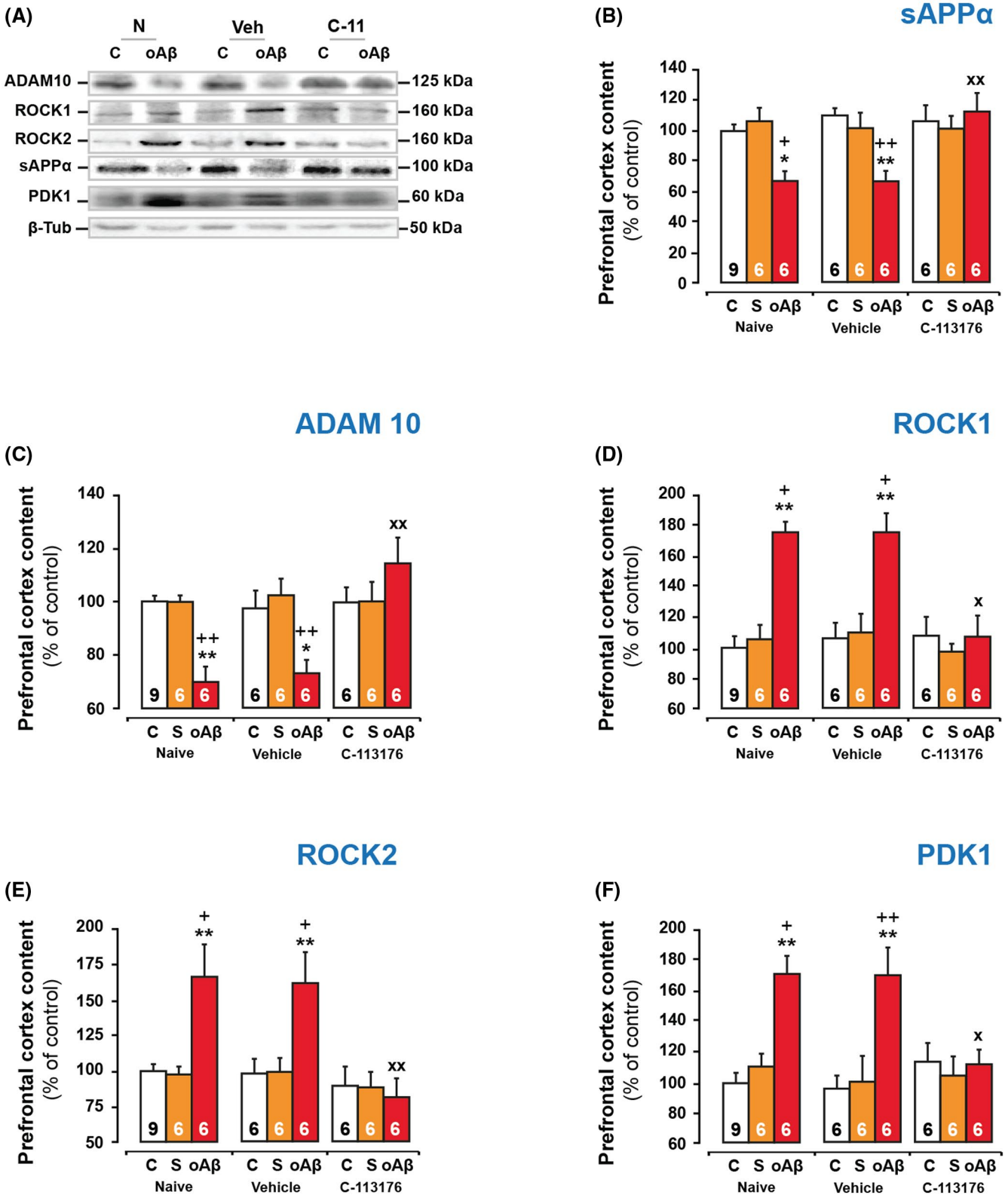

FIGURE 6 The effects in the PFC of selective GR modulator on the non-amyloidogenic pathways (A) modulated by the icv injection of oAβ_{25-35} were evaluated by Western blot. Variations of sAPPα (100 kDa) (A,B), ADAM10 (α-secretase, 70 kDa) (A,C), Rho-associated coiled-coil kinases (ROCK1 & ROCK2, 160 kDa) (A,D,E), and 3-phosphoinositide-dependent kinase (PDK1, 60 kDa) (A,F) were evaluated in control (C—white column) and in icv injected rats with 10 μg/rat of scrambled peptide (S—orange column) or oAβ_{25-35} (Aβ—red column), treated or not with vehicle (sesame oil) or selective GR modulator, CORT113176 (10 mg/kg per ip injection). For experimental protocol, see Figure 1A. The variations of sAPPα, ADAM10, ROCK1, ROCK2, and PDK1 in the PFC were normalized with the variations of β-tubulin (β-tub, 50 kDa) and compared with non-injected rats (control group: C). Two-way ANOVA: *sAPPα*: $F_{2,49} = 8.65$ for group, $P < .001$; $F_{2,49} = 3.92$ for treatment, $P < .05$; and $F_{4,49} = 4.25$ for interaction, $P < .01$; *ADAM10*: $F_{2,48} = 6.56$ for group, $P < .01$; $F_{2,48} = 7.07$ for treatment, $P < .01$; and $F_{4,48} = 7.08$ for interaction, $P < .001$; *ROCK1*: $F_{2,31} = 16.1$ for group, $P < .0001$; $F_{2,31} = 4.11$ for treatment, $P < .05$; and $F_{4,31} = 3.30$ for interaction, $P < .05$; *ROCK2*: $F_{2,51} = 10.5$ for group, $P < .001$; $F_{2,51} = 7.23$ for treatment, $P < .01$; and $F_{4,51} = 3.77$ for interaction, $P < .01$; *PDK1*: $F_{2,50} = 15.9$ for group, $P < .0001$; $F_{2,50} = 1.55$ for treatment, ns; and $F_{4,50} = 4.76$ for interaction, $P < .01$. The variations are expressed as means ± SEM in % of control values. *$P < .05$ and **$P < .01$ vs respective control (C) group. $^{+}P < .05$ and $^{++}P < .01$ vs respective scrambled (S) group. $^{x}P < .05$ and $^{xx}P < .01$ vs respective naive rat in each group (C, S or Aβ)

(*directly via GSK-3β and Cdk5 and indirectly via Fyn and Calpain 1*), which in turn increases the activation of these key enzymes and the HSP90/HSP70 ratio, worsening the AD pathogenesis[44-46] (Figure 7).

Our current data show that the seeding and the accumulation of endogenous Aβ induced by the icv injection of oAβ_{25-35}[43] (Figure S3B), not only results from the activation of amyloid pathways but also from the inhibition of non-amyloid pathways. Indeed, the icv injection of oAβ_{25-35} provoked the activation of the amyloidogenic pathway in the PFC, through an increase in Aβ synthesis (*APP/C99, Aβ_{1-42}, BACE1, and PS1 upregulation*) and a decrease in Aβ clearance (*IDE downregulation*), as previously reported for the hippocampus.[14] Besides, Aβ oligomers also inhibit the non-amyloidogenic pathway (*sAPPα and ADAM 10 downregulation*) and that this effect could be controlled by the activation of ROCK1 and ROCK2 (Figure 7). We showed that the oAβ_{25-35} injection-induced inhibition of sAPPα and ADAM10 is associated with an activation of ROCK/PDK1 pathways. These results are consistent with several studies showing that ROCKs modulate the shedding of sAPPα through an inhibition of tumor necrosis factor-α-converting enzyme (TACE or ADAM) activity, and that ROCKs depletion reduces Aβ levels.[68,75,76] ROCK activity seems to be directly upregulated by GC,[72,73,77] and ROCK/PDK1 activation after oAβ_{25-35} is reversed by treatment with CORT113176, again constituting a vicious cycle based on feed-forward effects on GR signaling (Figure 7).

ROCK also affect Tau hyperphosphorylation.[69,70] They activate the two principal enzymes involved in Tau phosphorylation, Cdk5 and GSK-3β.[71,78] In addition, ROCK/PDK1 inhibition of sAPPα may affect Tau, since it was shown that sAPPα reduces GSK-3β-mediated Tau phosphorylation.[79] These two mechanisms again link GR and GC to the pathophysiology of AD (Figure 7). Likewise, Tau phosphorylation may also be directly impacted by the other GR-related enzymes we described. Indeed, Fyn can directly phosphorylate Tau on tyrosine residues.[80] Fyn can also directly activate GSK-3β to rapidly induce Tau phosphorylation in human neuroblastoma cells.[57] In the same line of evidence, it appears that Fyn controls the activity of PDK1 through an upregulation of ROCK,[81,82] and thus could also participate in the inhibition of the non-amyloidogenic pathway. Calpain 1 also activates GSK-3β and Cdk5, promoting Tau phosphorylation and Tau-associated neurodegeneration.[49,50] Calpain 1 can cleave the neuron-specific Cdk5 activator p35 to produce p25, which accumulates in the brains of AD patients.[52] In fact, it was shown that induction of p25 by Calpain 1 causes prolonged activation and mislocalization of Cdk5 and that the p25/Cdk5 kinase hyperphosphorylates Tau, disrupts the cytoskeleton and promotes the apoptotic death of primary cortical neurons.[55] Thus, Fyn and Calpain 1 upregulations may be involved in both the increased Tau phosphorylation after oAβ_{25-35} injection,[13] and in the activity of GSK-3β, Cdk5, and the processing of APP. This highlights the potential link that GR activation could play between Aβ and Tau (Figure 7).

The mechanisms by which GR affects the multiple enzymes identified here is unclear. GR are nuclear receptors that directly interact with specific genes *via* binding to glucocorticoid response element (GRE), interactions with other transcription factors, or *via* non-genomic mechanisms, such as epigenetic modifications.[5,82,83] A GRE has been described in the promoter regions of APP and BACE1.[84-86] For the other proteins, no mechanism of transcriptional regulation *via* GR has been identified. A recent study on hippocampal slices pre-treated with an inhibitor of transcription activity showed a non-genomic activation of GSK-3β by GC.[87] The efficacy of the sGRm suggests that it is able to antagonize also non-genomic GR signaling. Of note, involvement of membrane-localized GR was linked to AD not only for the regulation of GSK-3β[88] but also—surprisingly—in the regulation of BACE1.[89] For the other proteins, further investigations will be needed to decipher which mechanisms are involved in GR regulatory activity. There is also the potential for more indirect mechanisms, since membrane-localized GR can facilitate glutamatergic transmission,[90-92] affect some of the factors that we identified here *via* stimulation of excitotoxicity pathways.[8]

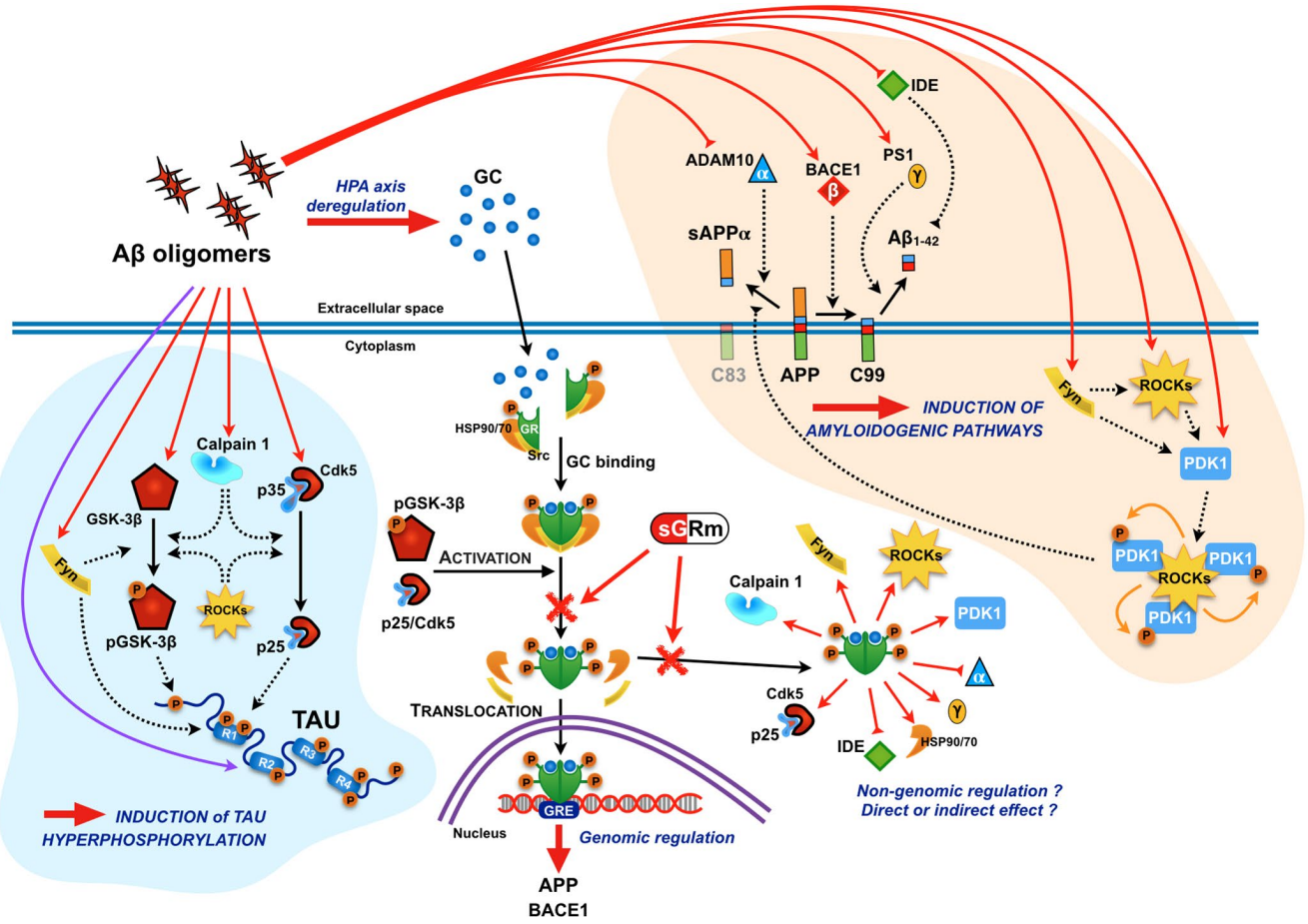

FIGURE 7 Schematic figure recapitulating the central role of GR and the therapeutic potential of selective GR modulators in AD. The icv injection of Aβ oligomers increases APP, C99 PS1, and BACE-1 contents, concomitantly with a decrease in IDE, evidencing the induction of the amyloidogenic pathway and, as previously observed, $A\beta_{1-42}$ production[42] and Tau hyperphosphorylation.[13] In parallel, the icv injection of Aβ oligomers inhibits sAPPα and ADAM10, evidencing the inhibition of non-amyloidogenic pathway. Aβ oligomers induce, in addition to an excess of circulating GC, an overactivation of GR, which is associated with an increase in the two main chaperones (HSP90 & HSP70) particularly involved in the activity of GR[43] but also in the control of Aβ and Tau aggregation.[44-46] Thus, active GR translocate to the nucleus where they exert their genomic effects through GRE, inducing APP and BACE-1 gene transcription, and potentiating Aβ oligomers production. Therefore, it evidences a first intracellular vicious cycle by which pathology increases circulating GC, which, in turn, increase pathology. Aβ oligomers also enhance contents and activity of key enzymes involved directly (Cdk5 and GSK-3β) or indirectly (Calpain 1 and Fyn) in the activation of GR but also in the hyperphosphorylation of Tau. Enzyme inductions which are regulated by GR, as evidenced after treatment with the selective GR modulator (CORT113176), demonstrate non-genomic effects of GR and thus a second intracellular vicious cycle. Indeed, pathology increases the activation of GR *via* several keys enzymes (Cdk5, GSK-3β, Calpain 1, and Fyn), which, in turn, increase the activation of these enzymes involved in the pathophysiology of AD. Finally, it appears that amyloid toxicity inhibits also the non-amyloidogenic pathways, reinforcing the displacement of the equilibrium in favor of endogenous amyloid seeding and evidencing another intracellular loop by which pathology increases the activation of GR, which, in turn, increases the activation of ROCKs/PDK1 pathways, as evidenced after treatment with the selective GR modulator (*CORT113176*). This activation accentuates the pathology through the inhibition of α-secretase (ADAM10) and sAPPα synthesis, as previously reported[79] but also by increasing the phosphorylation of Tau.[69-71,78] Red arrow: showed in this study. Purple arrow: showed in our previous studies.[13,65] Black arrow: known in the literature (*See discussion for references*). Blue arrow: hypothesis to assess. Red cross: Schematic effects of sGRm. AD, Alzheimer's disease; ADAM10, a disintegrin and metalloproteinase domain-containing protein 10 (*α-secretase*); APP, amyloid precursor protein; Aβ, amyloid-β peptide; BACE-1, β-APP cleaving enzyme (*β-secretase*); Cdk5, cyclin-dependent kinase-5; GC, glucocorticoids; GR, glucocorticoid receptors; GRE, glucocorticoid responsive element; GSK-3β, glycogen synthase kinase 3-β; HSP, heat-shock protein; IDE, insulin-degrading enzyme; PDK1, 3-phosphoinositide-dependent kinase; PS1, presenilin 1 (*γ-secretase*); ROCKs, Rho-associated coiled-coil kinases; sGRm, selective GR modulator (CORT113176)

This new study provides new arguments supporting the development of a vicious cycle based on GR activation in AD, here based on analysis of changes in the PFC. In this preclinical study, the new sGRm (CORT113176) blocked this cycle and normalized all AD processes analyzed, including extracellular (ADAM10, BACE1 and IDE),

intramembrane (PS1), and intracellular enzymes (Cdk5/p25, GSK-3β, Fyn, Calpain 1, ROCKs, and PDK1). In addition, we cannot exclude, as previously mentioned in the hippocampus,[14] the involvement of MR in the effects observed after sGRm treatment. Indeed, several studies suggested a neuroprotective role of these receptors in a context of GR blockade.[93-95] Thus, further investigations are needed to decipher the precise role of MR in the pathophysiology of AD. We moreover demonstrated that the accumulation of endogenous Aβ, induced by the amyloid toxicity and the concomitant dysregulation of HPA axis, resulted from the activation of amyloidogenic and the inhibition of the non-amyloidogenic pathways (Figure 7). All of these data place HPA axis dysregulation and GR in a central and crucial position in the pathophysiology of AD, linking amyloid toxicity and Tau deregulation. This work also highlights the therapeutic potential of sGRm to counteract negative effects induced by the amyloid toxicity and to re-establish the functionality of GR and a fortiori to re-establish the primal role of GC in the maintenance of homeostasis.

ACKNOWLEDGMENTS

The authors are thankful to Elisabeth HUETTER and the animal facility staff (CECEMA, University of Montpellier, France) for their daily assistance. They also particularly thank Corcept Therapeutics for generously providing glucocorticoid receptor ligand. Parts of this study were supported by INSERM, University of Montpellier, and EPHE annual resources (France), by a grant from "France Alzheimer" and "Fédération pour la Recherche sur le Cerveau" (*Grant AAP SM2016#1512 - LG*), by a grant from the "Agence Nationale de la Recherche" (*ANR*) under the program "Investissements d'Avenir" (*ANR-11-LABEX-0021-LipSTIC - CD*) and by a grant from Corcept Therapeutics (*Menlo Park, CA, USA*; *Exceptional subvention - LG*). G. CANET is supported by a PhD Grant from the University of Montpellier, France (*CBS2 PhD program*). C. HERNANDEZ is supported by a PhD Grant from the University of Montpellier, France (*CBS2 PhD program*).

CONFLICT OF INTEREST

JKB and HH are employees of Corcept Therapeutics (*Menlo Park, CA, USA*), which develops GR ligands for clinical use. Corcept Therapeutics provided compounds and financed part of the experiments. However, they are not involved in the experimental design, results analysis, and conclusions of the present study. All other authors declare that they have no competing interests.

AUTHOR CONTRIBUTIONS

G. Canet, F. Pineau, C. Hernandez, and C. Zussy performed experiments. H. Hunt and J.K. Belanoff provided glucocorticoid receptor ligand tested in this study. G. Canet, F. Pineau, C. Zussy, C. Hernandez, C. Desrumaux, N. Chevallier, V. Perrier, J. Torrent, H. Hunt, O. Meijer, and J.K. Belanoff corrected the manuscript. L. Givalois designed the study, wrote the protocol (with the help of G. Canet), performed part of experiments, analyzed the data (with the help of C. Desrumaux, N. Chevallier, and O. Meijer), and wrote the manuscript with G. Canet. All authors read and approved the final manuscript. All funders had no role in data collection, analysis, or in the writing of the manuscript.

REFERENCES

1. Selkoe DJ. Alzheimer's disease: genes, proteins, and therapy. *Physiol Rev*. 2001;81:741-766.
2. Querfurth HX, Laferla FM. Alzheimer's disease. *N Engl J Med*. 2010;362:329-444.
3. Hartmann A, Veldhuis JD, Deuschle M, Standhardt H, Heuser I. Twenty-four hour cortisol release profiles in patients with Alzheimer's and Parkinson's disease compared to normal controls: ultradian secretory pulsatility and diurnal variation. *Neurobiol Aging*. 1997;18:285-289.
4. Hoogendijk WJ, Meynen G, Endert E, Hofman MA, Swaab DF. Increased cerebrospinal fluid cortisol level in Alzheimer's disease is not related to depression. *Neurobiol Aging*. 2006;7:780.e1-780.e2.
5. Reul JM, De Kloet ER. Two receptor systems for corticosterone in rat brain: microdistribution and differential occupation. *Endocrinology*. 1985;117:2505-2511.
6. Roozendaal B. Glucocorticoids and the regulation of memory consolidation. *Psychoneuroendocrinology*. 2000;25:213-238.
7. Jankord R, Herman JP. Limbic regulation of hypothalamo-pituitary-adrenocortical function during acute and chronic stress. *Ann NY Acad Sci*. 2008;1148:64-73.
8. McEwen BS. Central effects of stress hormones in health and disease: understanding the protective and damaging effects of stress and stress mediators. *Eur J Pharmacol*. 2008;583:174-185.
9. Green K, Billings L, Roozendaal B, McGaugh J, LaFerla FM. Glucocorticoids increase amyloid-beta and tau pathology in a mouse model of Alzheimer's disease. *J Neurosci*. 2006;26:9047-9056.
10. Rothman SM, Herdener N, Camandola S, et al. 3xTgAD mice exhibit altered behavior and elevated Aβ after chronic mild social stress. *Neurobiol Aging*. 2012;33:830.e1-830.e12.
11. Lesuis SL, Weggen S, Baches S, Lucassen PJ, Krugers HJ. Targeting glucocorticoid receptors prevents the effects of early life stress on amyloid pathology and cognitive performance in APP/PS1 mice. *Transl Psychiatry*. 2018;8:53.
12. Zussy C, Brureau A, Delair B, et al. Time-course and regional analyses of the physiopathological changes induced after cerebral injection of an amyloid-β fragment in rats. *Amer J Pathol*. 2011;179:315-334.
13. Zussy C, Brureau A, Keller E, et al. Alzheimer's disease related markers, cellular toxicity and behavioral deficits induced six weeks after oligomeric amyloid-β peptide injection in rats. *PLoS One*. 2013;8:e531117.
14. Pineau F, Canet G, Desrumaux C, et al. New selective glucocorticoid receptor modulators reverse amyloid-β peptide-induced hippocampus toxicity. *Neurobiol Aging*. 2016;45:109-122.
15. Brureau A, Zussy C, Delair B, et al. Deregulation of HPA axis functions in an Alzheimer's disease rat model. *Neurobiol Aging*. 2013;34:1426-1439.

16. Catania C, Sotiropoulos I, Silva R, et al. The amyloidogenic potential and behavioral correlates of stress. *Mol Psychiatry*. 2009;14:95-105.
17. Baglietto-Vargas D, Medeiros R, Martinez-Coria H, LaFerla FM, Green KN. Mifepristone alters amyloid precursor protein processing to preclude amyloid beta and also reduces tau pathology. *Biol Psychiatry*. 2013;74:357-366.
18. Notarianni E. Hypercortisolemia and glucocorticoid receptor-signaling insufficiency in Alzheimer's disease initiation and development. *Curr Alzheimer Res*. 2013;10:714-731.
19. Lanté F, Chafai M, Raymond EF, et al. Subchronic glucocorticoid receptor inhibition rescues early episodic memory and synaptic plasticity deficits in a mouse model of Alzheimer's disease. *Neuropsychopharmacology*. 2015;40:1772-1781.
20. Sullivan RM, Gratton A. Prefrontal cortical regulation of hypothalamic-pituitary-adrenal function in the rat and implications for psychopathology: side matters. *Psychoneuroendocrinology*. 2002;27:99-114.
21. Davidson RJ. Anxiety and affective style: role of prefrontal cortex and amygdala. *Biol Psychiatry*. 2002;51:68-80.
22. Braak H, Braak E. Evolution of the neuropathology of Alzheimer's disease. *Acta Neurol Scand Suppl*. 1996;165:3-12.
23. Diorio D, Viau V, Meaney MJ. The role of the medial prefrontal cortex (cingulate cortex) in the regulation of hypothalamic-pituitary-adrenal responses to stress. *J Neurosci*. 1993;13:3839-3847.
24. Clark RD, Ray NC, Williams K, et al. 1H-Pyrazolo(3,4-g)hexahydro-isoquinolines as selective glucocorticoid receptor antagonists with high functional activity. *Bioorg Med Chem Lett*. 2008;18:1312-1317.
25. Beaudry J, Dunford EC, Teich T, et al. Effects of selective and non-selective glucocorticoid receptor II antagonists on rapid-onset diabetes in young rats. *PLoS One*. 2014;9:e91248.
26. Hunt H, Belanoff JK, Golding E, et al. 1H-Pyrazolo(3,4-g)hexahydro-isoquinolines as potent GR antagonists with reduced hERG inhibition and an improved pharmacokinetic profile. *Bioorg Med Chem Lett*. 2015;25:5720-5725.
27. Zalachoras I, Houtman R, Atucha E, et al. Differential targeting of brain stress circuits with a selective glucocorticoid receptor modulator. *Proc Natl Acad Sci USA*. 2013;110:7910-7915.
28. Meijer O, Koorneef LL, Kroon J. Glucocorticoid receptor modulators. *Ann Endocrinol*. 2018;79:107-111.
29. Solomon MB, Wulsin AC, Rice T, et al. The selective glucocorticoid receptor antagonist CORT 108297 decreases neuroendocrine stress responses and immobility in the forced swim test. *Horm Behav*. 2014;65:363-371.
30. Meyer M, Lara A, Hunt H, et al. The selective glucocorticoid receptor modulator CORT113176 reduces neurodegeneration and neuroinflammation in Wobbler mice spinal cord. *Neuroscience*. 2018;384:384-396.
31. Kaneko I, Morimoto K, Kubo T. Drastic neuronal loss in vivo by beta-amyloid racemized at Ser(26) residue: conversion of non-toxic [D-Ser(26)]beta-amyloid 1–40 to toxic and proteinase-resistant fragments. *Neuroscience*. 2001;104:1003-1011.
32. Kubo T, Nishimura S, Kumagae Y, Kaneko I. In vivo conversion of racemized beta-amyloid ([D-Ser 26]A beta 1–40) to truncated and toxic fragments ([D-Ser 26]A beta 25–35/40) and fragment presence in the brains of Alzheimer's patients. *J Neurosci Res*. 2002;70:474-483.
33. Gruden MA, Davidova TB, Malisauskas M, et al. Differential neuroimmune markers to the onset of Alzheimer's disease neurodegeneration and dementia: autoantibodies to Abeta((25–35)) oligomers, S100b and neurotransmitters. *J Neuroimmunol*. 2007;186:181-192.
34. Fung J, Frost D, Chakrabartty A, McLaurin J. Interaction of human and mouse Abeta peptides. *J Neurochem*. 2004;91:1398-1403.
35. Pike CJ, Burdick D, Walencewicz AJ, Glabe CG, Cotman CW. Neurodegeneration induced by beta-amyloid peptides in vitro: the role of peptide assembly state. *J Neurosci*. 1993;13:1676-1687.
36. Pike CJ, Walencewicz-Wasserman AJ, Kosmoski J, Cribbs DH, Glabe CG, Cotman CW. Structure-activity analyses of beta-amyloid peptides: contributions of the beta 25–35 region to aggregation and neurotoxicity. *J Neurochem*. 1995;64:253-265.
37. Yamada K, Nabeshima T. Animal models of Alzheimer's disease and evaluation of anti-dementia drugs. *Pharmacol Ther*. 2000;88:93-113.
38. Yankner BA, Duffy LK, Kirschner DA. Neurotrophic and neurotoxic effects of amyloid beta protein: reversal by tachykinin neuropeptides. *Science*. 1990;250:279-282.
39. Varadarajan S, Kanski J, Aksenova M, Lauderback C, Butterfield DA. Different mechanisms of oxidative stress and neurotoxicity for Alzheimer's A beta(1–42) and A beta(25–35). *J Am Chem Soc*. 2001;123:5625-5631.
40. Selkoe DJ, Hardy J. The amyloid hypothesis of Alzheimer's disease at 25 years. *EMBO Mol Med*. 2016;8:595-608.
41. Paxinos G, Watson C. *The Rat Brain in Stereotaxic Coordinates*. 3rd ed. San Diego, CA: Academic Press; 1997.
42. Meunier J, Villard V, Givalois L, Maurice T. The γ-secretase inhibitor2-[(1R)-1-((4-chlorophenyl)sulfonyl) (2,5-difluorophenyl) amino)ethyl-5-fluorobenzenebutanoic acid (BMS-299897] alleviates Aβ1-42 seeding and short-term memory deficits in the Aβ25-35 mouse model of Alzheimer's disease. *Eur J Pharmacol*. 2013;698:193-199.
43. Kirschke E, Goswami D, Southworth D, Griffin PR, Agard DA. Glucocorticoid receptor function regulated by coordinated action of the Hsp90 and Hsp70 chaperone cycles. *Cell*. 2014;157:1685-1697.
44. Dou F, Netzer WJ, Tanemura K, et al. Chaperones increase association of tau protein with microtubules. *Proc Natl Acad Sci USA*. 2003;100:721-726.
45. Chen Y, Wang B, Liu D, et al. Hsp90 chaperone inhibitor 17-AAG attenuates Aβ-induced synaptic toxicity and memory impairment. *J Neurosci*. 2014;34:2464-2470.
46. Lackie RE, Maciejewski A, Ostapchenko VG, et al. The Hsp70/Hsp90 chaperone machinery in neurodegenerative diseases. *Front Neurosci*. 2017;11:254.
47. Wang Z, Frederick J, Garabedian MJ. Deciphering the phosphorylation "code" of the glucocorticoid receptor in vivo. *J Biol Chem*. 2002;277:26573-26580.
48. Galliher-Beckley AJ, Cidlowski JA. Emerging roles of glucocorticoid receptor phosphorylation in modulating glucocorticoid hormone action in health and disease. *IUBMB Life*. 2009;61:979-986.
49. Beurel E, Grieco SF, Jope RS. Glycogen synthase kinase-3 (GSK3): regulation, actions, and diseases. *Pharmacol Ther*. 2015;148:114-131.
50. Sun LH, Ban T, Liu CD, et al. Activation of Cdk5/p25 and tau phosphorylation following chronic brain hypoperfusion in rats involves microRNA-195 down-regulation. *J Neurochem*. 2015;134:1139-1151.
51. Naert G, Ferré V, Meunier J, et al. Leucettine L41, a DYRK1A-preferential DYRKs/CLKs inhibitor, prevents memory impairments

and neurotoxicity induced by oligomeric Aβ25-35 peptide administration in mice. *Eur Neuropsychopharmacol*. 2015;25:2170-2182.
52. Patrick GN, Zukerberg L, Nikolic M, de la Monte S, Dikkes P, Tsai LH. Conversion of p35 to p25 deregulates Cdk5 activity and promotes neurodegeneration. *Nature*. 1999;402:615-6223.
53. Kurbatskaya K, Phillips EC, Croft CL, et al. Upregulation of calpain activity precedes tau phosphorylation and loss of synaptic proteins in Alzheimer's disease brain. *Acta Neuropathol Commun*. 2016;4:34.
54. Jin N, Yin X, Yu D, et al. Truncation and activation of GSK-3β by calpain 1: a molecular mechanism links to tau hyperphosphorylation in Alzheimer's disease. *Sci Rep*. 2015;5:8187.
55. Lee MS, Kwon YT, Li M, Peng J, Friedlander RM, Tsai LH. Neurotoxicity induces cleavage of p35 to p25 by calpain. *Nature*. 2000;405:360-364.
56. Oakley RH, Cidlowski JA. The biology of the glucocorticoid receptor: new signaling mechanisms in health and disease. *J Allergy Clin Immunol*. 2013;132:1033-1044.
57. Lesort M, Jope RS, Johnson GV. Insulin transiently increases tau phosphorylation: involvement of glycogen synthase kinase-3beta and Fyn tyrosine kinase. *J Neurochem*. 1999;72:576-584.
58. Löwenberg M, Tuynman J, Bilderbeek J, et al. Rapid immunosuppressive effects of glucocorticoids mediated through Lck and Fyn. *Blood*. 2005;106:1703-1710.
59. Li XH, Liu NB, Zhang MH, et al. Effects of chronic multiple stress on learning and memory and the expression of Fyn, BDNF, TrkB in the hippocampus of rats. *Chin Med J*. 2007;120:66974.
60. García-Rojo G, Gámiz F, Ampuero E, et al. In vivo sub-chronic treatment with dichlorvos in young rats promotes synaptic plasticity and learning by a mechanism that involves acylpeptide hydrolase instead of acetylcholinesterase inhibition. Correlation with endogenous β-amyloid levels. *Front Pharmacol*. 2017;8:483.
61. Lin D, Cao L, Wang Z, Li J, Washington JM, Zuo Z. Lidocaine attenuates cognitive impairment after isoflurane anesthesia in old rats. *Behav Brain Res*. 2012;228:319-327.
62. Chang J, Xie M, Shah VR, et al. Activation of Rho-associated coiled-coil protein kinase 1 (ROCK-1) by caspase-3 cleavage plays an essential role in cardiac myocyte apoptosis. *Proc Natl Acad Sci USA*. 2006;103:14495-14500.
63. Loirand G. Rho kinases in health and disease: from basic science to translational research. *Pharmacol Rev*. 2015;67:1074-1095.
64. Swanger SA, Mattheyses AL, Gentry EG, Herskowitz JH. ROCK1 and ROCK2 inhibition alters dendritic spine morphology in hippocampal neurons. *Cell Logist*. 2016;5:e1133266.
65. Alleaume-Butaux A, Nicot S, Pietri M, et al. Double-edge sword of sustained ROCK activation in prion diseases through neuritogenesis defects and prion accumulation. *PLoS Pathog*. 2015;11:e1005073.
66. Lai AY, McLaurin J. Rho-associated protein kinases as therapeutic targets for both vascular and parenchymal pathologies in Alzheimer's disease. *J Neurochem*. 2018;144:659-668.
67. Hu YB, Zou Y, Huang Y, et al. ROCK1 is associated with Alzheimer's disease-specific plaques, as well as enhances autophagosome formation but not autophagic Aβ clearance. *Front Cell Neurosci*. 2016;10:253.
68. Pietri M, Dakowski C, Hannaoui S, et al. PDK1 decreases TACE-mediated α-secretase activity and promotes disease progression in prion and Alzheimer's diseases. *Nat Med*. 2013;19:1124-1131.
69. Amano M, Kaneko T, Maeda A, et al. Identification of Tau and MAP2 as novel substrates of Rho-kinase and myosin phosphatase. *J Neurochem*. 2003;87:780-790.
70. Gentry EG, Henderson BW, Arrant AE, et al. Rho kinase inhibition as a therapeutic for progressive supranuclear palsy and corticobasal degeneration. *J Neurosci*. 2016;36:1316-1323.
71. Castro-Alvarez JF, Gutierrez-Vargas J, Darnaudéry M, Cardona-Gómez GP. ROCK inhibition prevents tau hyperphosphorylation and p25/CDK5 increase after global cerebral ischemia. *Behav Neurosci*. 2011;125:465-472.
72. Huang GX, Wang Y, Su J, et al. Up-regulation of Rho-associated kinase 1/2 by glucocorticoids promotes migration, invasion and metastasis of melanoma. *Cancer Lett*. 2017;410:1-11.
73. Rubenstein NM, Callahan JA, Lo DH, Firestone GL. Selective glucocorticoid control of Rho kinase isoforms regulate cell-cell interactions. *Biochem Biophys Res Commun*. 2007;354:603-607.
74. Ho GJ, Hashimoto M, Adame A, et al. Altered p59Fyn kinase expression accompanies disease progression in Alzheimer's disease: implications for its functional role. *Neurobiol Aging*. 2005;26:625-635.
75. Herskowitz JH, Feng Y, Mattheyses AL, et al. Pharmacologic inhibition of ROCK2 suppresses amyloid-β production in an Alzheimer's disease mouse model. *J Neurosci*. 2013;33:19086-19098.
76. Henderson BW, Gentry EG, Rush T, et al. Rho-associated protein kinase 1 (ROCK1) is increased in Alzheimer's disease and ROCK1 depletion reduces amyloid-β levels in brain. *J Neurochem*. 2016;138:525-531.
77. Liu D, Xiong R, Chen X, et al. The glucocorticoid dexamethasone inhibits U937 cell adhesion and neutrophil release via RhoA/ROCK1-dependent and independent pathways. *Cell Physiol Biochem*. 2014;33:1654-1662.
78. Hamano T, Yen SH, Gendron T, Ko LW, Kuriyama M. Pitavastatin decreases Tau levels via the inactivation of Rho/ROCK. *Neurobiol Aging*. 2012;33:2306-2320.
79. Deng J, Habib A, Obregon DF, et al. Soluble amyloid precursor protein alpha inhibits tau phosphorylation through modulation of GSK3β signaling pathway. *J Neurochem*. 2015;135:630-637.
80. Scales TM, Derkinderen P, Leung KY, et al. Tyrosine phosphorylation of tau by the Src family kinases Lck and Fyn. *Mol Neurodegener*. 2011;6:12.
81. Liu DZ, Sharp FR, Van KC, et al. Inhibition of SRC family kinases protects hippocampal neurons and improves cognitive function after traumatic brain injury. *J Neurotrauma*. 2014;3:1268-1276.
82. Lv Z, Hu M, Ren X, et al. Fyn mediates high glucose-induced actin cytoskeleton reorganization of podocytes via promoting ROCK activation in vitro. *J Diabetes Res*. 2016;2016:5671803.
83. Gray JD, Kogan JF, Marrocco J, McEwen BS. Genomic and epigenomic mechanisms of glucocorticoids in the brain. *Nat Rev Endocrinol*. 2017;13:661-673.
84. Lahiri DK. Functional characterization of amyloid beta precursor protein regulatory elements: rationale for the identification of genetic polymorphism. *Ann NY Acad Sci*. 2004;1030:282-288.
85. Sambamurti K, Kinsey R, Maloney B, Ge YW, Lahiri DK. Gene structure and organization of the human beta-secretase (BACE) promoter. *FASEB J*. 2004;18:1034-1036.
86. Laping NJ, Nichols NR, Day JR, Johnson SA, Finch CE. Transcriptional control of glial fibrillary acidic protein and glutamine synthetase in vivo shows opposite responses to corticosterone in the hippocampus. *Endocrinology*. 1994;135:1928-1933.
87. Dey A, Hao S, Wosiski-Kuhn M, Stranahan AM. Glucocorticoid-mediated activation of GSK3β promotes tau phosphorylation and impairs memory in type 2 diabetes. *Neurobiol Aging*. 2017;57:75-83.

88. Jozic I, Vukelic S, Stojadinovic O, et al. Stress signals, mediated by membranous glucocorticoid receptor, activate PLC/PKC/GSK-3β/β-catenin pathway to inhibit wound closure. *J Invest Dermatol*. 2017;137:1144-1154.
89. Choi GE, Lee SJ, Lee HJ, Ko SH, Chae CW, Han HJ. Membrane-associated effects of glucocorticoid on BACE1 upregulation and Aβ generation: involvement of lipid Raft-mediated CREB activation. *J Neurosci*. 2017;37:8459-8476.
90. Groeneweg FL, Karst H, de Kloet ER, Joëls M. Rapid non-genomic effects of corticosteroids and their role in the central stress response. *J Endocrinol*. 2011;209:153-167.
91. Groeneweg FL, Karst H, de Kloet ER, Joëls M. Mineralocorticoid and glucocorticoid receptors at the neuronal membrane, regulators of nongenomic corticosteroid signalling. *Mol Cell Endocrinol*. 2012;350:299-309.
92. Popoli M, Yan Z, McEwen BS, Sanacora G. The stressed synapse: the impact of stress and glucocorticoids on glutamate transmission. *Nat Rev Neurosci*. 2011;13:22-37.
93. Almeida OF, Condé GL, Crochemore C, et al. Subtle shifts in the ratio between pro- and antiapoptotic molecules after activation of corticosteroid receptors decide neuronal fate. *FASEB J*. 2000;14:779-790.
94. Crochemore C, Lu J, Wu Y, et al. Direct targeting of hippocampal neurons for apoptosis by glucocorticoids is reversible by mineralocorticoid receptor activation. *Mol Psy*. 2005;10:790-798.
95. Le Menuet D, Lombès M. The neuronal mineralocorticoid receptor: from cell survival to neurogenesis. *Steroids*. 2014;91:11-19.

SUPPORTING INFORMATION

Additional supporting information may be found online in the Supporting Information section.

How to cite this article: Canet G, Pineau F, Zussy C, et al. Glucocorticoid receptors signaling impairment potentiates amyloid-β oligomers-induced pathology in an acute model of Alzheimer's disease. *The FASEB Journal*. 2020;34:1150–1168. https://doi.org/10.1096/fj.201900723RRR